An interactive meta-analysis of MRI biomarkers of myelin

Matteo Mancini[1,2,3], Agah Karakuzu[2], Julien Cohen-Adad[2,4], Mara Cercignani[1,5], Thomas Nichols[6,7,*], Nikola Stikov[2,8,*]

1 – Department of Neuroscience, Brighton and Sussex Medical School, University of Sussex, Brighton, United Kingdom.
2 – NeuroPoly Lab, Polytechnique Montreal, Montreal, Quebec, Canada.
3 – CUBRIC, Cardiff University, Cardiff, United Kingdom.
4 – Functional Neuroimaging Unit, CRIUGM, Université de Montréal, Montreal, Quebec, Canada
5 – Neuroimaging Laboratory, Fondazione Santa Lucia, Rome, Italy.
6 – Wellcome Centre for Integrative Neuroimaging (WIN FMRIB), University of Oxford, Oxford, United Kingdom.
7 – Big Data Institute, University of Oxford, Oxford, United Kingdom.
8 – Montreal Heart Institute, Université de Montréal, Montreal, Quebec, Canada.

* These authors contributed equally to this work.

Abstract

Several MRI measures have been proposed as in vivo biomarkers of myelin, each with applications ranging from plasticity to pathology. Despite the availability of these myelin-sensitive modalities, specificity and sensitivity have been a matter of discussion. Debate about which MRI measure is the most suitable for quantifying myelin is still ongoing. In this study, we performed a systematic review of published quantitative validation studies to clarify how different these measures are when compared to the underlying histology. We analysed the results from 43 studies applying meta-analysis tools, controlling for study sample size and using interactive visualization (https://neurolibre.github.io/myelin-meta-analysis). We report the overall estimates and the prediction intervals for the coefficient of determination and find that MT and relaxometry-based measures exhibit the highest correlations with myelin content. We also show which measures are, and which measures are not statistically different regarding their relationship with histology.

Abbreviations and mathematical symbols

AD – axial diffusivity

AK – axial kurtosis

AWF – axonal water fraction

FA – fraction anisotropy

ihMTR – inhomogeneous magnetization transfer ratio

k_fm – free water-macromolecular exchange rate

k_mf – macromolecular-free water exchange rate

M0m – macromolecular pool magnetization fraction

MD – mean diffusivity

MK – mean kurtosis

MPF – macromolecular pool fraction

MT – magnetization transfer

MTR – magnetization transfer ratio

MTR-UTE – magnetization transfer ratio (using ultra-short echo time)

MTV – macromolecular tissue volume

MVF-MT – myelin volume fraction (estimated from MT)

MVF-T2 – myelin volume fraction (estimated from T2)

MWF – myelin water fraction

PD – proton density

PN – peripheral nerve

PRISMA – Preferred Reporting Items for Systematic Reviews and Meta-Analyses

QSM – quantitative susceptibility mapping

R1f – free water pool longitudinal relaxation rate

R2* – apparent transverse relaxation rate

RAFF – relaxation along a fictitious field

RD – radial diffusivity

RD-DBSI – radial diffusivity (from diffusion basis spectrum imaging)

RDe – extra-cellular compartment radial diffusivity

RK – radial kurtosis

rSPF – relative semi-solid proton fraction

SC – spinal cord

T1 – longitudinal relaxation time

T1p – adiabatic longitudinal relaxation time

T1sat – longitudinal relaxation time under magnetization transfer irradiation

T2 – transverse relaxation time

T2f – free water pool transverse relaxation time

T2int – transverse relaxation intermediate component

T2m – macromolecular pool transverse relaxation rate

T2p – adiabatic transverse relaxation time

Introduction

Myelin is a key component of the central nervous system. The myelin sheaths insulate axons with a triple effect: allowing fast electrical conduction, protecting the axon, and providing trophic support (Nave & Werner, 2014). The conduction velocity regulation has become an important research topic, with evidence of activity-dependent myelination as an additional mechanism of plasticity (Fields, 2015; Sampaio-Baptista & Johansen-Berg, 2017). Myelin is also relevant from a clinical perspective, given that demyelination is often observed in several neurological diseases such as multiple sclerosis (Höftberger & Lassmann, 2018).

Given this important role in pathology and plasticity, measuring myelin in vivo has been an ambitious goal for magnetic resonance imaging (MRI) for more than two decades (A. Mackay et al., 1994; Rooney et al., 2007; G.J. Stanisz, Kecojevic, Bronskill, & Henkelman, 1999). Even though the thickness of the myelin sheath is in the order of micrometres, well beyond the MRI spatial resolution, its presence influences several physical properties that can be probed with MRI, from longitudinal and transversal relaxation phenomena to water molecule diffusion processes.

However, being sensitive to myelin is not enough: to study how and why myelin content changes, it is necessary to define a specific biomarker. Interestingly, the quest for measuring myelin has evolved in parallel with an important paradigm shift in MRI research, where MRI data are no longer treated as just “pictures”, but as actual 3D distributions of quantitative measures. This perspective has breathed new life into an important field of research, quantitative MRI (qMRI), that encompasses the study of how to measure the relevant electromagnetic properties that influence magnetic resonance phenomena in biological tissues (Cercignani, Dowell, & Tofts, 2018; Cohen-Adad & Wheeler-Kingshott, 2014). From the very definition of qMRI, it is clear that its framework applies to any approach for non-invasive myelin quantification.

Similarly to other qMRI biomarkers, MRI-based myelin measurements are indirect, and might be affected by other microstructural features, making the relationship between these indices and myelination noisy. Assessing the accuracy of such measurements, and their sensitivity to change, is essential for their translation into clinical applications. Validation is therefore a fundamental aspect of their development (Cohen-Adad, 2018). The most common approach is based on acquiring MR data

from in vivo or ex vivo tissue and then comparing those data with the related samples analysed using histological techniques. Despite being the most realistic approach, this comparison involves several methodological choices, from the specific technique used as a reference to the quantitative measure used to describe the relationship between MRI and histology. So far, a long list of studies have looked at MRI-histology comparisons (Cohen-Adad, 2018; Laule & Moore, 2018; A. L. MacKay & Laule, 2016; Petiet et al., 2019), each of them focusing on a specific pathology and a few MRI measures.

Despite these numerous studies, there is still an ongoing debate on what MRI measure should be used to quantify myelin and as a consequence there is a constant methodological effort to propose new measures. This debate would benefit from a quantitative analysis of all the findings published so far, specifically addressing inter-study variations and prospects for future studies, something that is currently missing from the literature.

In this study, we systematically reviewed quantitative MRI-histology comparisons and we used meta-analysis tools to address the following question: how different are the modalities for myelin quantification in terms of their relationship with the underlying histology?

Results

Literature survey

The screening process is summarized in the flowcharts in Figure 1 and Figure A1. The keywords as reported in the appendix returned 688 results on PubMed (last search on 03/06/2020). These results included 50 review articles. From the 50 review articles, six were selected as relevant for both the topics of myelin and related MRI-histology comparisons (Cohen-Adad, 2018; Laule & Moore, 2018; Laule et al., 2007; A. L. MacKay & Laule, 2016; Petiet et al., 2019; Turner, 2019). After the assessment, 58 original research studies were considered eligible, as shown in Table A1 (in the appendix) and Figure S2. All the data collected are available in the supplementary materials.

In terms of specific modalities, the survey shows that the most common MRI approach compared with histology was diffusion-weighted imaging (used in 28 studies), followed

by magnetization transfer (MT, 27 studies), T2 relaxometry (19 studies) and T1 relaxometry (10 studies). Only 20 studies considered more than one approach: among the others, 20 focused exclusively on diffusion, 12 on MT, and 6 on T2 relaxometry.

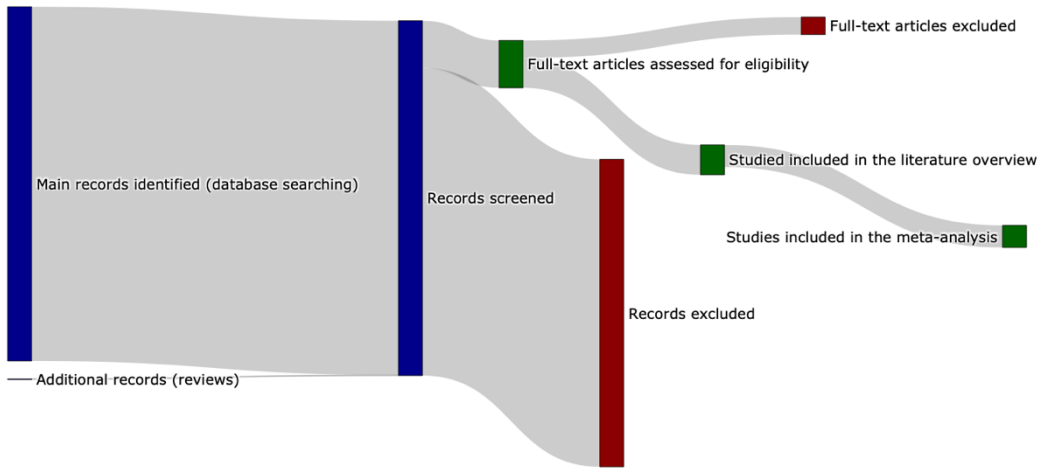

Figure 1 – Sankey diagram representing the screening procedure (PRISMA flow chart provided in the appendix). To see the interactive figure: https://neurolibre.github.io/myelin-meta-analysis/01/selection.html#figure-1

From these 58 studies, we then focused only on brain studies and we further excluded studies not reporting either the number of subjects or the number of ROIs per subject. We also excluded one single-subject study that relied on voxels as distinct samples, whereas the other studies in this review are based on ROIs (i.e. including more than one voxel). In the end, 43 suitable studies were identified for the subsequent analyses.

Meta-analysis

To compare the studies of interest, we first organized them according to the MRI measure used. Figure 2 and Figure 3 (and also Figure S3-S4) show the R^2 values for the selected studies across measures: the highest values (R^2>0.8) are obtained mostly from MT measures, but they are associated with small sample sizes (with an average of 32 sample points). The studies with largest sample sizes are associated with R^2 values between 0.6 and 0.8 for MT and T2 relaxometry, but with lower values for T1 relaxometry and other approaches.

To combine the results for each measure, we then used a mixed-effect model: in this way we were able to express the overall effect size in terms of a range of R^2 values

within a confidence interval, but also to assess prediction intervals and inter-study differences. The results are shown as forest plots in Figure 4 (and also Figure S5).

Apart from MPF and MWF, all the measures showed R^2 overall estimates in the range 0.21-0.53. To investigate the significance of the differences between measures, we conducted a repeated measures meta-regression on every R^2 estimate recorded (98 in total over 43 studies). As shown in Figure 5 (and also Figure S6), the measures can be roughly subdivided in two groups: MT- and relaxometry-based measures gave significantly higher R^2 estimates compared to diffusion-based measures. Within the diffusion-based measures, FA shows slightly higher estimates than the others, with marginal significance over RD and AD or no significance in case of MD.

Within MT- and relaxometry-based measures, the trends follow those in the forest plots (Figure 4), but most differences are not significant (Figure 5). However, the results in terms of z-score give a measure of distance between the R^2 distributions. From this perspective, MPF has higher R^2 estimates compared to all the other measures, but it is only marginally higher than MWF (z-score=0.77; p-value=1) so we cannot claim that one is superior to the other. Following the same reasoning, MTR and T1 are not statistically different (z-score=0.47; p-value=1).

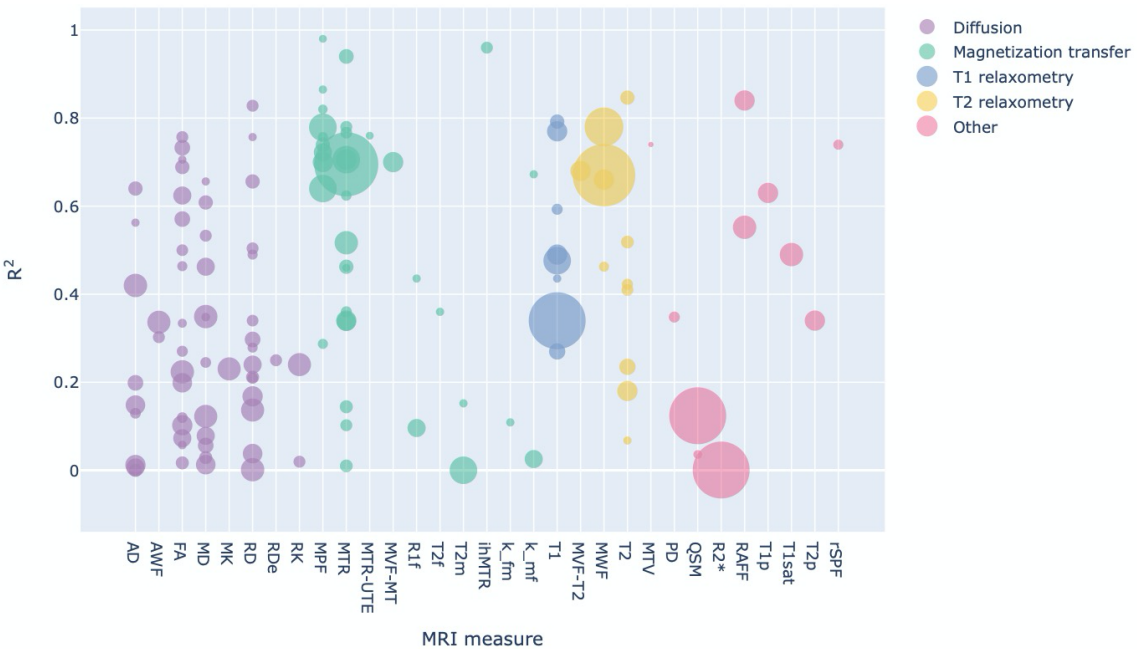

Figure 2 – Bubble chart of R^2 values between a given MRI measure and histology for each study across MRI measures, with the area proportional to the number of samples. To see the interactive figure: https://neurolibre.github.io/myelin-meta-analysis/02/closer_look.html#figure-3

When considering the prediction intervals calculated using τ^2 (the variance of the effect size parameters across the population of studies), for most measures the interval spanned from 0.1 to 0.9 (Figure 4 and Figure S5). This implies that future studies relying on such measures can expect, on the basis of these studies, to obtain any R^2 value in this broad interval. The only exceptions were MPF (0.49-1) and MWF (0.45-0.95), whose intervals were narrower than the alternatives. Finally, I^2 (a measure of how much of the variability in a typical study is due to heterogeneity in the experimental design) was generally quite high (Table 1). MWF showed the lowest I^2 across measures (I^2=73.19%), but this may be misleading considering that it was based on only 4 studies while the other measures included around 10 studies. Excluding MWF, MPF also showed a relatively low I^2 (I^2=83.18%). Qualitative comparisons across experimental conditions and methodological choices highlighted differences across pathology models, targeted tissue types and reference techniques (Figure 6 and Figure S7). Other factors such as magnetic field, co-registration, specific tissue and the related conditions (Figure S8) showed comparable distributions.

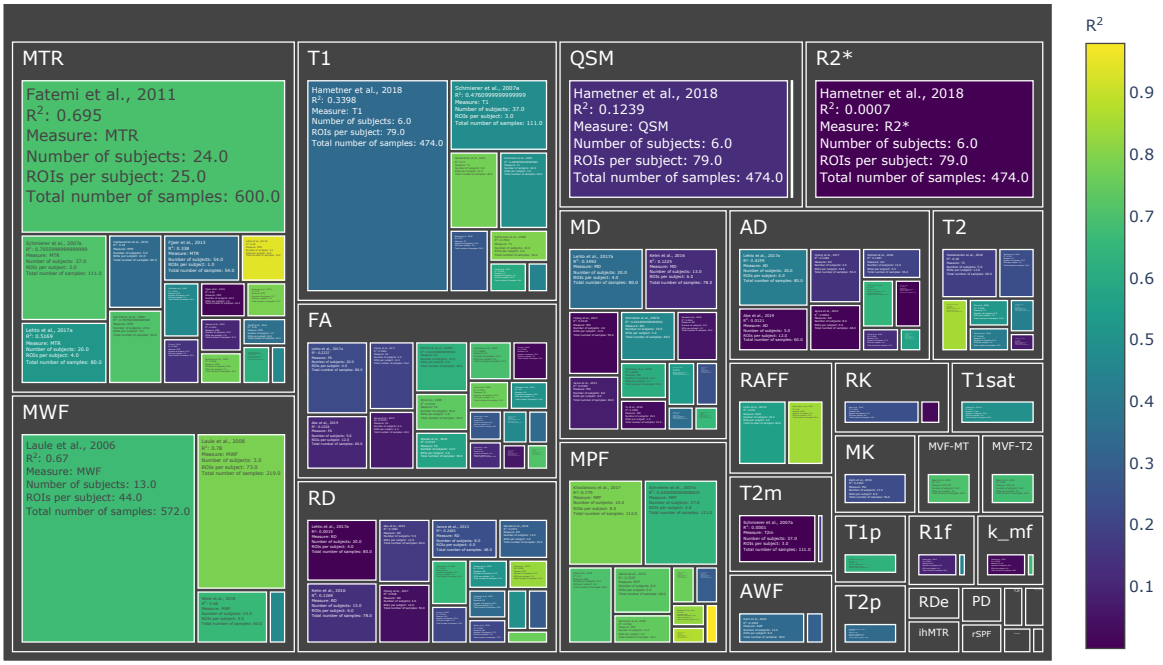

Figure 3 – Treemap chart of the studies considered for the meta-analysis, organized by MRI measure. The color of each box represents the reported R^2 value while the size box is proportional to the sample size. To see the interactive figure: https://neurolibre.github.io/myelin-meta-analysis/02/closer_look.html#figure-4

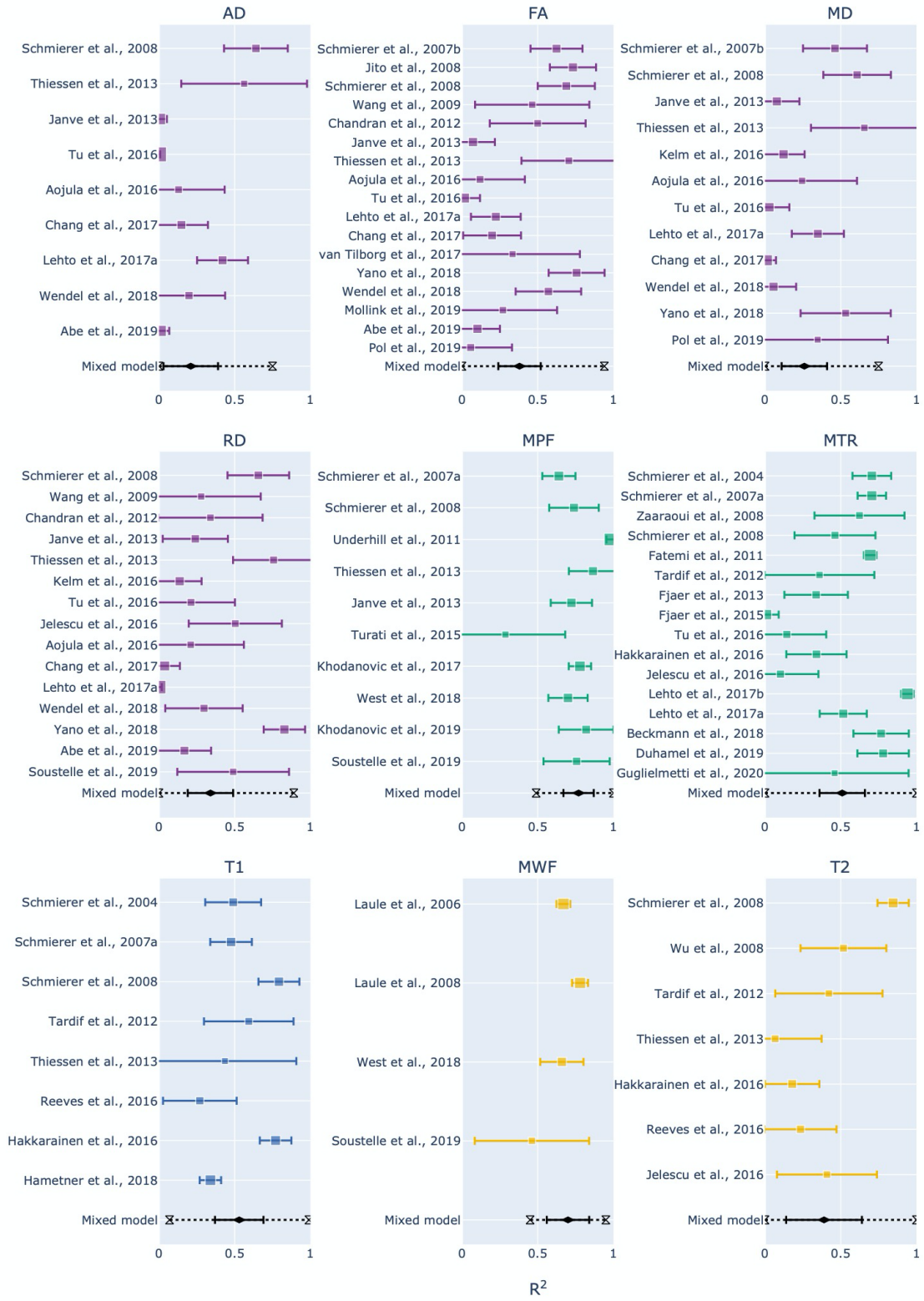

Figure 4 – Forest plots showing the R^2 values reported by the studies and estimated from the mixed-effect model for each measure. The hourglasses and the dotted lines in the mixed-effect model outcomes represent the prediction intervals.
To see the interactive figure: https://neurolibre.github.io/myelin-meta-analysis/03/meta_analysis.html#figure-5

Discussion

Indirect measures are the most popular (for better or worse)

The literature survey offers an interesting perspective on popular research trends (Figure S2). The first consideration one can make is that every myelin imaging technique achieves myelin sensitivity through different means. A clear example is offered by the two most common approaches in this meta-analysis, DWI and MT: the MT effect is driven by saturation pulses interacting with myelin macromolecules that transfer their magnetization to water, whereas in diffusion experiments myelin is just not part of the picture. Diffusion acquisitions are blind to direct myelin measurement because the TEs used are too long (~100ms) to be influenced by the actual macromolecules – with T2 of ~10us (G.J. Stanisz et al., 1999) – or even the water molecules trapped in the myelin sheath – with T2 of ~30ms (A. Mackay et al., 1994). To infer myelin content, one needs to rely on the interaction between intra-cellular and extra-cellular water compartments. The majority of diffusion studies included in this analysis used tensor-based measures (with fractional anisotropy being the most common), but some also used kurtosis-based analysis. The main issue with this approach is that other factors affect those measures (Beaulieu, 2002, 2009), making it difficult to specifically relate changes in water compartments to changes in myelin.

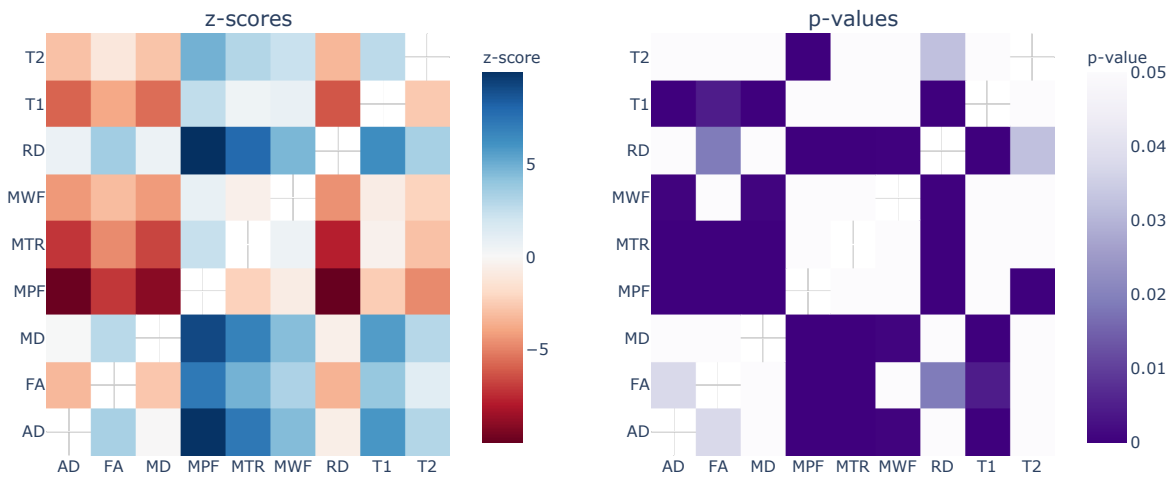

Figure 5 – Results from the repeated measures meta-regression, displayed in terms of z-scores (left) and p-values (right) for each pairwise comparison across all the MRI measures. In the z-score heatmap, each element refers to the comparison between the measure on the x axis with the one on the y axis. For example, MPF and FA (z-score=7.14; p-value<0.0001) are statistically different, while MPF and T1 (z-score=2.51; p-value=0.43) are not statistically different. To see the interactive figure: https://neurolibre.github.io/myelin-meta-analysis/03/meta_analysis.html#figure-6

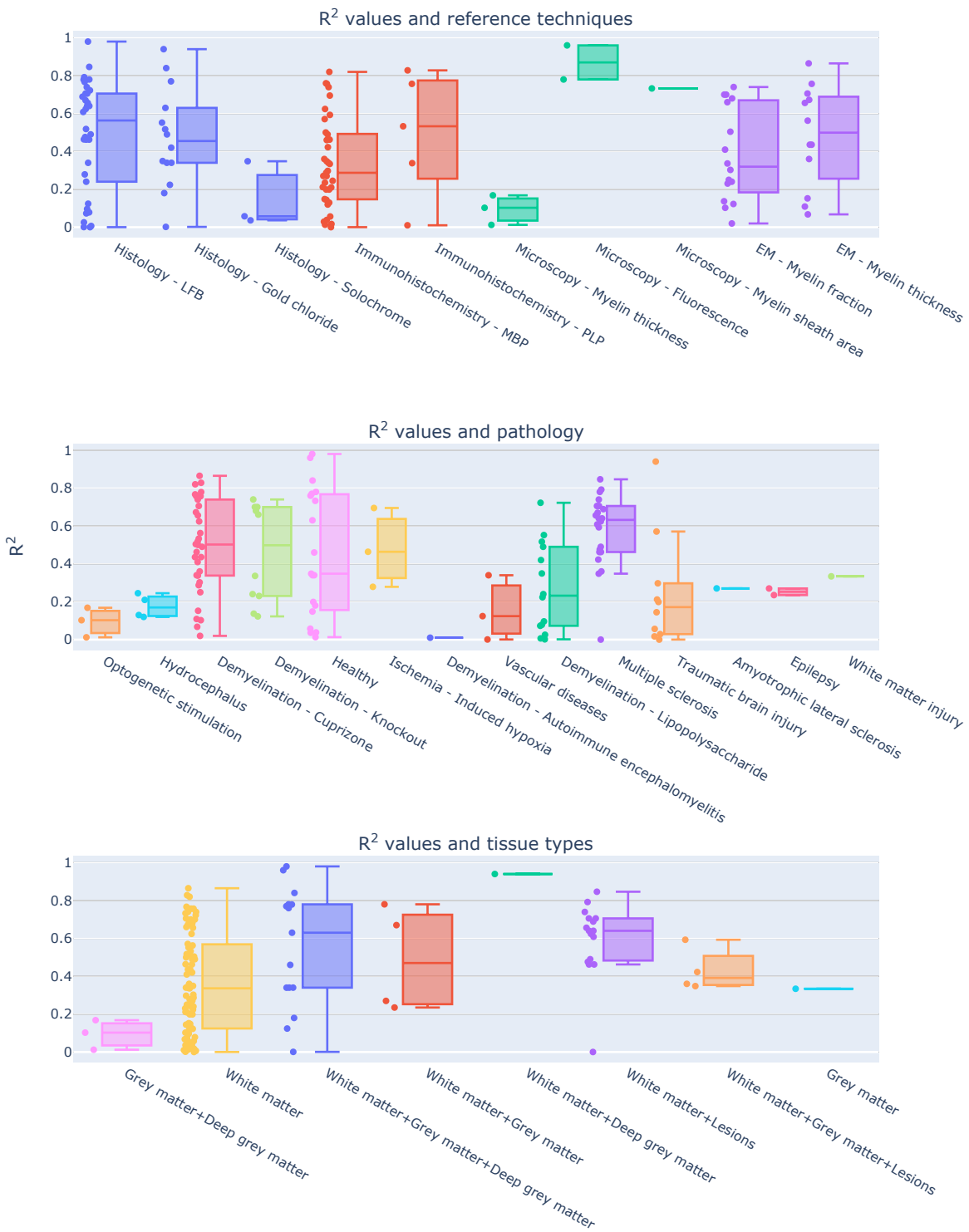

Figure 6 – Experimental conditions and methodological choices influencing the R^2 values (top: reference techniques; middle: pathology model; bottom: tissue types). To see the interactive figure: https://neurolibre.github.io/myelin-meta-analysis/04/other_factors.html#figure-7

MEASURE	NUMBER OF STUDIES	ESTIMATE	STANDARD ERROR	TAU²	I²
MTR	16	0.508	0.0691	0.07	96.03%
MPF	10	0.7657	0.0455	0.0128	83.18%
FA	17	0.3766	0.0663	0.0652	87.49%
RD	15	0.3364	0.0679	0.0615	92.30%
MD	12	0.2639	0.0679	0.044	87.35%
T1	8	0.5321	0.0692	0.0328	86.51%
AD	9	0.2095	0.0802	0.048	97.69%
T2	7	0.3938	0.1023	0.0651	84.49%
MWF	4	0.6997	0.0432	0.0041	73.19%

Table 1 Results from the mixed-effect models: for each measure we reported the number of studies, the estimate and standard error of the overall R^2 distribution, the τ^2 and the I^2.

Despite this issue, the use of diffusion as a proxy for myelin is quite widespread, specifically outside the field of quantitative MRI. This is probably a consequence of how popular DWI has become and how widely available are the related acquisition sequences. MT, the second most popular technique for quantifying myelin, estimates myelin by acquiring data with and without saturating the macromolecular proton pool. The simplest MT measure, MT ratio (MTR), incorporates non-myelin contributions in the final measurement. Recent acquisition variations include computing MTR from acquisitions with ultra-short echo times (Du, Takahashi, Bydder, Chung, & Bydder, 2009; Guglielmetti et al., 2020; Wei et al., 2018) or relying on inhomogeneous MT (Duhamel et al., 2019; Varma, Duhamel, de Bazelaire, & Alsop, 2015). More complex experiments, e.g. quantitative MT, are based on fitting two compartments to the data, the free water and the macromolecular compartments, or pools. In this way, one is able to assess myelin through MPF with higher specificity, although still potentially including contributions from other macromolecules. Additional measures have also been considered (including the T2 of each pool, the exchange rate between the pools). The drawback of qMT is the requirement for a longer and more complex acquisition. Recently there have been alternative techniques to estimate only MPF, resulting in faster acquisitions with similar results (M. Khodanovich et al., 2019; M. Y. Khodanovich et al., 2017; Yarnykh, 2012). Despite being focused on macromolecular contributions, these approaches are not strictly specific to myelin (Sled, 2018): in this sense, an important limitation is that MT effects are sensitive to the pH of the targeted tissue and

therefore changes in the pH (caused for example by inflammation processes) will affect MT-based measures of myelin (Greg J. Stanisz, Webb, Munro, Pun, & Midha, 2004).

Following diffusion and MT, the most popular approach is T2 relaxometry. Unlike diffusion and MT, in T2 relaxometry experiments one can directly observe the contribution from the water trapped between the myelin bilayers, and can therefore estimate the myelin water fraction. A simpler but less specific approach consists in estimating the transverse relaxation time considering the decay to be mono-exponential. A historical and practical drawback of these approaches is that they require longer acquisitions, although faster alternatives have been developed (Does & Gore, 2000; Prasloski et al., 2012). A more subtle but nevertheless important limitation lies in the multi-compartment model used in multi-exponential T2 relaxometry (Does, 2018): this model generally assumes slow water exchange between compartments, but it has been showed that water exchange actually contributes to T2 spectra variations (Dula, Gochberg, Valentine, Valentine, & Does, 2010; Kevin D. Harkins, Dula, & Does, 2012).

Finally, other studies used a diverse collection of other measures, including T1 relaxometry, apparent transversal relaxation rate (R2*), proton density (PD), macromolecular tissue volume (MTV), relaxation along a fictitious field (RAFF), and quantitative susceptibility mapping (QSM).

After this general overview, it is clear that each modality could be a suitable candidate for a quantitative myelin biomarker. To then make a choice informed by the studies here reported, it becomes necessary to consider not only effect sizes in terms of correlation, but also sample sizes and acquisition times.

<u>There is no myelin MRI measure true to histology</u>

When looking at the R^2 values across the different measures, the first detail that catches one's eye is how most measures present a broad range of values (Figure 2 and Figure 3). When taking into account the sample size, the largest studies show higher correlations for MT and T2 relaxometry studies than any other approach (Figure S3 and Figure S4). In quantitative terms, the meta-analysis corroborates this idea, showing that MPF and MWF tend to be more specific to myelin compared to the other

measures (respectively with R^2=0.7657 and R^2=0.6997), in line with the underlying theory. Notably, diffusion-based measures show the lowest overall estimates (with values between R^2=0.3766 for FA and R^2=0.2095 for AD): this could be due to the fact, as already mentioned, that DWI does not specifically measure myelin properties, and despite FA and RD being influenced by the myelin content, they are also influenced by other factors that make them unsuitable as measures of myelin. The repeated measure meta-regression confirms this overall picture, clearly distinguishing MT- and relaxometry-based measures from diffusion-based ones (Figure 5).

Despite these considerations on the advantages of MPF and MWF, one should refrain from concluding that they are the "true" MRI measures of myelin. The reason for this caution is given not by the overall effect sizes observed here, but by the collateral outcomes of the meta-analysis. The first one is given by the prediction intervals: most measures exhibit large intervals (Figure 4), not supporting the idea of them being robust biomarkers. MPF and MWF seem to be again the most suitable choices for future studies, but a range between 0.5 and 1 is still quite large.

The second important aspect to consider is given by the differences across studies: the meta-analysis showed how such differences strongly limit inter-study comparisons for a given measure (Figure 6). This result should be expected, given that the studies here examined are inevitably influenced by the specific experimental constraints and methodological choices. Given the limited number of studies, it is not possible to quantitatively study interactions between MRI measures and the other factors (e.g. modality used as a reference, tissue types, magnetic field strength). For further qualitative insights, we invite the reader to explore the interactive figures S7-S8. A first important factor to consider is the validation modality used as a reference, which will be dictated by the equipment availability and cost. However, such a choice has an impact on the actual comparison: histology and immunochemistry, despite being specific to myelin, do not offer a volumetric measure of myelin, but rather a proxy based on the transmittance of the histological sections. So far, the only modality able to give a volumetric measure would be electron microscopy, which is an expensive and resource-consuming approach. Also, electron microscopy has several limitations, including tissue shrinkage, degradation of the myelin sheath structure due to imperfect fixation, imperfect penetration of the osmium stain, polishing, keeping focus over large

imaging regions. All these effects contribute to the lack of precision and accuracy when quantifying myelin content with EM-based histology (Cohen-Adad, 2018). Another important observation is that none of the studies here reviewed considered histology reproducibility, which is hard to quantify as a whole given that a sample can be processed only once: collateral factors affecting tissue processing (e.g. sectioning distortions, mounting and staining issues) constitute an actual limitation for histology-based validation. A further example of influential factor often dictated by equipment availability is the magnetic field strength of the MRI scanner: figure S8 shows that most studies were conducted at 7T and 9.4T, with some pioneering studies at 1.5T and even fewer ones at other field strengths.

In addition to differences in experimental and methodological designs, there are also several considerations that arise out of the lack of shared practices in MRI validation studies. The first evident one is the use of correlations: despite being a simple measure that serves well the purpose of roughly characterizing a relationship, Pearson correlation is not the right tool for quantitative biomarkers, as it does not characterize the actual relationship between histology and MRI. Linear regression is a step forward but has the disadvantage of assuming a linear relationship. Despite Pearson correlation and linear regression being the most common measures used in the studies here reviewed, it is still not clear if the relationship is actually linear. Only one study among the considered ones computed both Pearson and Spearman correlation values (Tardif, Bedell, Eskildsen, Collins, & Pike, 2012), and reported higher Spearman correlations, pointing out that non-linear relationships should actually be considered. One last consideration regarding the use of correlation measures for validating quantitative biomarkers is about the intercept in the MRI-histology relationship. Notably, only MWF is expected to assume a value equal to zero when myelin is absent (West et al., 2018). For the other measures, it would be necessary to estimate the intercept, which leads to the calibration problem in the estimate of myelin volume fraction. Notably, calculating Pearson correlation does not provide any information for such calibration. Another arbitrary practice that would benefit from some harmonization is the choice of ROIs. The studies reported here examined a diverse list of ROIs, in most cases hand-drawn on each modality, encompassing different types of tissue, and the most common approach is to report a single, pooled

correlation. This is problematic, as different types of tissue (e.g. grey matter and white matter) will show different values for MRI-based measures but also for histology-based ones, making linearity assumptions about the two modalities. However, with this approach gross differences between tissues drive the observed correlation, without actually showing if the MRI-based measure under analysis is sensitive to subtle differences and therefore a suitable quantitative biomarker for myelin. The effect of considering different types of tissues is showed in Figure 6 and Figure S7, where correlation ranges change when considering different types of tissue. However, the large correlation range in white matter, the most common tissue studied, suggests that other factors also affect the correlation.

It should be clear at this point that any debate about a universal MRI-based measure of myelin is pointless, at least at the moment, as the overall picture provided by previous studies does not point to any such ideal measure. Nevertheless, is debating about a universal measure helpful for future studies?

Better biomarkers require more reproducibility studies

We hope this meta-analysis convinces the reader that a holy grail of myelin imaging does not exist, at least as long as we consider histology to be the ground truth. Given that we all have to pick our poison, the upside is that measures based on MT and relaxometry are not statistically different, and therefore future studies have an actual choice among candidate measures. For further progress, rather than debating about a perfect measure, we would argue that what is missing at the moment is a clear picture of what can be achieved with each specific MRI modality. The studies examined here focus on a large set of different measures, and more than half of them considered at most two measures, highlighting how the field is mostly focused on formulating new measures. While it is understood that novel measures can provide new perspectives, it is also fundamentally important to understand the concrete capabilities and limitations of current measures. From this meta-analysis, what the literature clearly lacks is reproducibility studies, specifically answering two main questions: (1) what is the specificity of each measure? We should have a practical validation of our theoretical understanding of the relevant confounds; (2) what is the "parameter sensitivity" of each measure? Here we refer to parameter sensitivity in a

broad sense, that includes also experimental conditions and methodological choices. The results here presented show how certain conditions (e.g. pathology) seem to affect the coefficient of determination more than others but given the limited number of studies for each modality, we refrained from additional analyses to avoid speculation. A warning message that is evident from these results is the inherent limitation of DWI for estimating myelin content: this is not by any means a novel result (Beaulieu, 2002, 2009), but it is nevertheless worth reiterating given the outcomes of our analysis. If estimating myelin content is relevant in a diffusion study, it is important to consider complementing the diffusion measure with one of the modalities here reviewed; in this way, it would be possible to decouple the influence of myelin content from the many other factors that come into play when considering diffusion phenomena.

Finally, an important factor to take into account when choosing a biomarker of myelin is the actual application. For animal research, long acquisitions are not a major issue. However, when considering biomarkers for potential clinical use, the acquisition time can become a relevant issue. An example is the well-established multi-echo spin-echo implementation of MWF, that can only be used for a specific slice in a hypothetical clinical scenario. Faster techniques have been proposed for estimating it with gradient- and spin-echo (GRASE) sequences (Does & Gore, 2000; Feinberg & Oshio, 1991; Prasloski et al., 2012). Even in this case, the acquisition time still reaches 15 minutes for acquiring roughly the whole brain with an isotropic resolution of 2mm. Complex MT acquisitions such as qMT suffer from the same problem, although it is possible to use optimized and faster protocols to focus specifically on MPF (M. Khodanovich et al., 2019; M. Y. Khodanovich et al., 2017; Yarnykh, 2012).

Conclusions

Several MRI measures are sensitive to myelin content and the current literature suggests that most of them are not statistically different in terms of their relationship with the underlying histology. Measures highly correlated with histology are also the ones with a higher expected specificity. This suggests that future studies should try to better address how specific each measure is, for the sake of clarifying suitable applications.

Methods

Review methodology

The Medline database (https://pubmed.ncbi.nlm.nih.gov) was used to retrieve the articles. The keywords used are specified in the appendix. We followed the PRISMA (Preferred Reporting Items for Systematic Reviews and Meta-Analyses) guidelines for record screening and study selection. The results were first screened to remove unrelated work. Specifically we discarded: work relying only on MRI; work relying only on histology or equivalent approaches; work reporting only qualitative comparisons. After this first screening, the remaining papers were assessed. At this stage, we discarded: studies using MRI-based measures in arbitrary units (e.g. T1-weighted or T2-weighted data); studies using measures of variation in myelin content (defined either as the difference between normal and abnormal myelin content) either for MRI or for histology; studies using arbitrary assessment scales; studies comparing MRI-based absolute measures of myelin with histology-based relative measures (e.g. g-ratio); studies reporting other quantitative measures than correlation or R^2 values; studies comparing histology from one dataset and MRI from a different one. As an additional source for potential candidate studies, we screened the review articles in the initial results, and we selected the relevant studies that were not already present in the studies already selected.

From the final papers, we collected first the following details: the DOI; which approach was used (diffusion, MT, T1 relaxometry, T2 relaxometry, or other); which specific MRI measures were compared to histology or equivalent techniques; the magnetic field; the technique used as a reference (histology, immunochemistry, microscopy, electron microscopy); the focus of the study in terms of brain, spinal cord or peripheral nerve; if the subjects were humans or animals, and if the latter which animal; if the tissue under exam was *in vivo*, *in situ* or *ex vivo*, and in the latter case if the tissue was fixed or not; if the tissue was healthy or pathological, and if the latter which pathology; the specific structures examined for correlation purposes; which comparison technique was used (e.g. Pearson correlation, Spearman correlation, linear regression); the number of subjects; the number of ROIs per subject; the male/female ratio; if registration procedures were performed to align MRI and histology; in case of pathological tissue, if control tissue was considered as well; other relevant notes. If

before calculating the correlations the data were averaged across subjects, the number of subjects was considered to be one. The same consideration was made for averaging across ROIs. This is because the numbers of subjects and ROIs were used to take into account how many sample points were used when computing the correlation. We set each of those numbers to 1 for all the studies where the data were averaged respectively across subjects and across ROIs. Finally, in those cases where the number of ROIs or the number of subjects were given as a range rather than specific values, we used the most conservative value and added the related details to the notes.

We then proceeded to collect the quantitative results reported for each measure and for each study in the form of R^2. Given that different studies may rely on a different strategy when reporting correlations, we adopted the following reasoning to limit discrepancies across studies while still objectively representing each of them. In case of multiple correlation values reported, for our analysis we selected the ones referring to the whole dataset and the entire brain if available, and considering each ROI in a given subject as a sample if possible; if only correlation values for specific ROIs were reported, the one for the most common reported structure would be chosen. In the case of multiple subjects, if data were provided separately for each group, the correlation for the control group was used. When different comparison methods were reported (e.g. both Pearson and Spearman correlation) or if the MRI data was compared with multiple references (e.g. both histology and immunohistochemistry), the correlations used were chosen on the basis of the following priority orders (from the most preferable to the least): for multiple comparison methods, linear regression, Spearman correlation, Pearson correlation; for multiple reference techniques, electron microscopy, immunohistochemistry, histology. Finally, in any other case where more than one correlation value was available, the most conservative value was used. Any other additional value was in any case mentioned in the notes of the respective study.

Meta-analysis

For the quantitative analysis, we restricted our focus on brain studies and only on the ones providing an indication of both the number of subjects and the number of ROIs. For each study, we computed the sample size as the product between the number of

subjects and the number of ROIs per subject. In this way, we were able to compare the reported R^2 values across measures taking into account the related number of points actually used for correlation purposes. We note that correlation or regression analyses run on multiple ROIs and subjects represents a repeated measures analysis, for which the degrees of freedom computation can be complex; however, most papers neglected the repeated measures structure of the data and thus the sample size computation here represents a very approximate and optimistic view of the precision of each R^2 value.

To estimate the variance of each R^2 value, we relied on the correlation properties and the delta method (Lehman, 1999). Let us consider the Pearson's correlation r of two variables X and Y with population correlation ρ. If r is calculated from N random samples, the sampling variance is $(1-\rho^2)^2/N$. Applying the delta method, we then approximated the variance of R^2 as $4R^2(1-R^2)^2/N$, assuming $R^2 \approx \rho^2$. As we recognise that some papers computed Spearman correlation, this calculation is again optimistic and may underestimate the sampling variability of the squared Spearman correlation.

To estimate the overall effect size in terms of R^2 we have to choose how to model the distribution of true effects given by the data collected from the literature. The two most common approaches are fixed-effects and mixed-effects models. While the underlying mathematical model is the same as the one used for linear regression (more details in the appendix), the assumptions are different: fixed-effects models assume that all the studies share a common effect size, while mixed-effects models assume that the effect size across studies is similar but not identical (Raudenbush, 2009). In our case, as the studies have several factors that influence the R^2 values (e.g. histology/microscopy reference, magnetic field strength, pathology model), we expect a distribution of effect sizes due to inter-study differences. This is why we proceeded to fit a mixed-effects model to each measure that was featured in more than two studies. Apart from the effect size distributions, we reported two additional measures, I^2 and tau^2: the former expresses as a percentage how much of variability in a typical study is due to heterogeneity (i.e. the variation in study outcomes between studies) rather than chance (Higgins & Thompson, 2002), while the latter can be used to calculate the prediction interval (Raudenbush, 2009), which gives the expected range for the measure of interest in future studies. We used forest plots to represent the

outcomes, and both the mixed effects estimate of the population estimated R^2, with both a 95% confidence and a (larger) 95% prediction interval.

For the explicit purpose of comparing the effect sizes between different MRI measures, we conducted a repeated measures meta-regression on every R^2 value recorded. We associated each R^2 value with three additional details: (i) the related variance, as done in the measure-specific mixed-effects models; (ii) the related study, used as the random intercept (i.e. random variable) to incorporate potential inter-study variability; and (iii) the related MRI measure, used as the moderator (i.e. categorical variable) to estimate the differences between measures. In this way, the meta-regression leads to R^2 intervals for each MRI measure, with the same trend as measure-specific mixed-effects models but with subtle differences. This is because the meta-regression makes two additional assumptions: first, R^2 estimates within the same study share the same random effects; and second, the between-study variance is the same for all observations. We then used the meta-regression R^2 estimates to compute every possible pairwise comparison between MRI measures and to identify significantly different pairs using Tukey's test, while controlling the error rate over all the possible comparisons (Bonferroni correction).

This additional model is necessary, as direct comparisons are not possible with measure-specific analyses. While the repeated measures meta-regression makes direct comparisons straightforward, we reported the main R^2 estimates based on the measure-specific mixed-effects models, as they make weaker assumptions.

For visual comparisons, we used the Jupyter notebook provided in the supplementary materials. For model fitting and forest plots, we used the Metafor package, version 2.4-0 (Viechtbauer, 2010).

Acknowledgements

MM was funded by the Wellcome Trust through a Sir Henry Wellcome Postdoctoral Fellowship [213722/Z/18/Z].

Appendix

Search keywords:

(myelin[Title/Abstract] AND ((magnetic[Title/Abstract] AND resonance[Title/Abstract]) OR mr[Title/Abstract] OR mri[Title/Abstract])) AND (histology[Title/Abstract] OR histopathology[Title/Abstract] OR microscopy[Title/Abstract] OR immunohistochemistry[Title/Abstract] OR histological[Title/Abstract] OR histologically[Title/Abstract] OR histologic[Title/Abstract] OR histopathological[Title/Abstract] OR histopathologically[Title/Abstract] OR histopathologic[Title/Abstract])

Results obtained from the Medline database: 688 (03/06/2020)

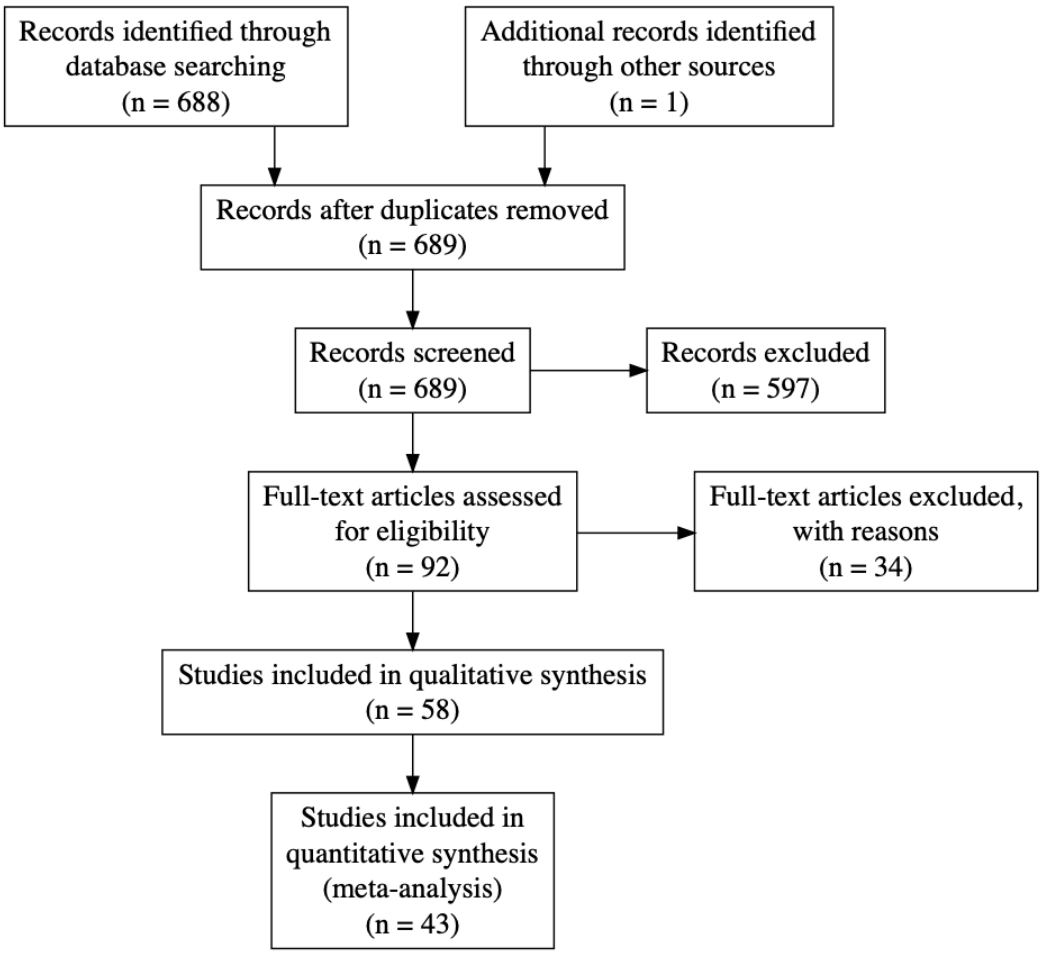

Figure A1 - PRISMA flowchart for the meta-analysis.

Fixed- and mixed-effects models

While a traditional linear regression model estimates the error variance from residuals, in a fixed effects meta-analysis model, each paper's response and standard errors, as well as the error variance of the regression model can be directly computed from the supplied response standard deviations. Specifically, for a (non-meta) regression model we have the i-th response y_i modelled with covariate values x_i, $y_i = x_i\beta + \varepsilon_i$, where random error has unknown variance $\mathrm{Var}(\varepsilon_i) = \sigma^2$. In a fixed-effects meta-analysis, we are given y_i but also s_i, the standard error of y_i, and the regression model has the same form except the variance is known, $\mathrm{Var}(\varepsilon_i) = s_i^2$, and the weighted least squares regression can be computed, estimating beta and its standard error. A mixed-effects meta-analysis accounts for more variance than what can be ascribed to the sampling error of the reported outcome. The regression model has again the same form, except now the variance is $\mathrm{Var}(\varepsilon_i) = s_i^2 + \tau^2$, the sum of the reported squared standard error and the unknown between-study variance τ^2. Iterative methods are used to estimate τ^2 and, once estimated, a weighted least squares regression can be computed. The parameter τ^2 can be interpreted as the variance of *noise-free* (hypothetical, zero standard error) results from the population of all possible studies. The importance of τ^2 can also be gauged by I^2, the proportion of variance due to random inter-study differences (i.e. $1 - I^2$ is the proportion attributable to random sampling error of each study) (Higgins & Thompson, 2002).

Table A1 - Selected studies for qualitative analysis.

Study	MRI measure(s)	Histology/microscopy measure	Tissue	Condition	Focus
(Schmierer, Scaravilli, Altmann, Barker, & Miller, 2004)	T1, MTR	Histology - LFB	Human	Multiple sclerosis	Brain
(Odrobina, Lam, Pun, Midha, & Stanisz, 2005)	T1, T2, T2int, MWF, M0m, MTR	Microscopy - Myelin fraction	Animal - Rat	Demyelination - Tellurium	PN
(Pun et al., 2005)	T1, T2int, MWF	Microscopy - Myelin fraction	Animal - Rat	Demyelination - Tellurium	PN
(Laule et al., 2006)	MWF	Histology - LFB	Human	Multiple sclerosis	Brain
(Schmierer, Tozer, et al., 2007)	T1, MTR, MPF, T2m	Histology - LFB	Human	Multiple sclerosis	Brain
(Schmierer, Wheeler-Kingshott, et al., 2007)	FA, MD	Histology - LFB	Human	Multiple sclerosis	Brain
(Jito et al., 2008)	FA	Microscopy - Myelin sheath area	Animal - Mouse	Healthy	Brain
(Kozlowski et al., 2008)	MWF, FA, AD, RD, MD	Immunohistochemistry - MBP	Animal - Rat	Injury - Dorsal columnar transection	SC
(Laule et al., 2008)	MWF	Histology - LFB	Human	Multiple sclerosis	Brain

(Schmierer et al., 2008)	T1, T2, MTR, MPF, MD, FA, AD, RD	Histology - LFB	Human	Multiple sclerosis	Brain
(Wu et al., 2008)	T2	Histology - LFB	Animal - Mouse	Demyelination - Cuprizone	Brain
(Zaaraoui et al., 2008)	MTR	Immunohistochemistry - MBP	Animal - Mouse	Demyelination - Cuprizone	Brain
(Takagi et al., 2009)	FA, AD	EM - Myelin thickness	Animal - Rat	Degeneration - Contusive injury	PN
(S. Wang et al., 2009)	FA, RD	Histology - LFB	Animal - Rat	Ischemia - Induced hypoxia	Brain
(Zhang et al., 2009)	RD	Histology - LFB	Animal - Rat	Injury - Dorsal columnar transection	SC
(Schmierer et al., 2010)	MTR, T2	Histology - LFB	Human	Multiple sclerosis	Brain
(Fatemi et al., 2011)	MTR	Immunohistochemistry - MBP	Animal - Mouse	Ischemia - Induced hypoxia	Brain
(Laule et al., 2011)	MWF	Immunohistochemistry - MBP	Human	Multiple sclerosis	Brain
(Underhill, Rostomily, Mikheev, Yuan, & Yarnykh, 2011)	MPF	Histology - LFB	Animal - Mouse	Healthy	Brain
(Chandran et al., 2012)	FA, RD	Immunohistochemistry - MBP	Animal - Mouse	Demyelination - Cuprizone	Brain

(Tardif et al., 2012)	T1, T2, MTR, PD	Immunohistochemistry - MBP	Human	Multiple sclerosis	Brain
(Fjaer et al., 2013)	MTR	Immunohistochemistry - PLP	Animal - Mouse	Demyelination - Cuprizone	Brain
(K. D. Harkins, Valentine, Gochberg, & Does, 2013)	MWF, MPF	Microscopy - Myelin fraction	Animal - Rat	Edema - Hexaclorophene	SC
(Janve et al., 2013)	MPF, R1a, k_ba, FA, RD, MD, AD	Histology - LFB	Animal - Rat	Demyelination - Lipopolysaccharide	Brain
(Thiessen et al., 2013)	MPF, R1f, k_fm, k_mf, T2f, T2m, MD, RD, AD, FA, T1, T2	EM - Myelin thickness	Animal - Mouse	Demyelination - Cuprizone	Brain
(Kozlowski, Rosicka, Liu, Yung, & Tetzlaff, 2014)	MWF	Immunohistochemistry - MBP	Animal - Rat	Injury - Dorsal columnar transection	SC
(X. Wang et al., 2014)	RD, RD-DBSI	Immunohistochemistry - MBP	Animal - Mouse	Demyelination - Autoimmune encephalomyelitis	SC
(Fjaer, Bo, Myhr, Torkildsen, & Wergeland, 2015)	MTR	Immunohistochemistry - PLP	Animal - Mouse	Demyelination - Autoimmune encephalomyelitis	Brain

(Seehaus et al., 2015)	FA, RD, MD	Histology - Silver	Human	Healthy	Brain
(Turati et al., 2015)	MPF	Immunohistochemistry - MBP	Animal - Mouse	Demyelination - Cuprizone	Brain
(Y. Wang et al., 2015)	RD-DBSI	Histology - LFB	Human	Multiple sclerosis	SC
(Aojula et al., 2016)	FA, AD, RD, MD	Immunohistochemistry - MBP	Animal - Rat	Hydrocephalus	Brain
(Hakkarainen et al., 2016)	T1, T2, MTR, T1p, T2p, RAFF	Histology - Gold chloride	Animal - Rat	Healthy	Brain
(Jelescu et al., 2016)	RD, RK, AWF, Rde, T2, MTR	EM - Myelin fraction	Animal - Mouse	Demyelination - Cuprizone	Brain
(Kelm et al., 2016)	MD, RD, MK, RK, AWF	EM - Myelin fraction	Animal - Mouse	Demyelination - Knockout	Brain
(Reeves et al., 2016)	T1, T2	Immunohistochemistry - MBP	Human	Epilepsy	Brain
(Tu et al., 2016)	FA, AD, RD, MD, MTR	Immunohistochemistry - MBP	Animal - Rat	Traumatic brain injury	Brain
(Chang et al., 2017)	FA, AD, RD, MD	Immunohistochemistry - MBP	Animal - Mouse	Healthy	Brain
(Chen, Holmes, Liu, Tetzlaff, & Kozlowski, 2017)	MWF	EM - Myelin fraction	Animal - Rat	Injury - Dorsal columnar transection	SC

(M. Y. Khodanovich et al., 2017)	MPF	Histology - LFB	Animal - Mouse	Demyelination - Cuprizone	Brain
(Lehto, Albors, et al., 2017)	RAFF, MTR, T1sat, FA, MD, AD, RD	Histology - Gold chloride	Animal - Rat	Demyelination - Lipopolysaccharide	Brain
(Lehto, Sierra, & Grohn, 2017)	MTR	Histology - Gold chloride	Animal - Rat	Traumatic brain injury	Brain
(van Tilborg et al., 2018)	FA	Immunohistochemistry - MBP	Animal - Rat	White matter injury	Brain
(Beckmann et al., 2018)	MTR	Histology - LFB	Animal - Mouse	Demyelination - Cuprizone	Brain
(Berman, West, Does, Yeatman, & Mezer, 2018)	MTV	EM - Myelin fraction	Animal - Mouse	Demyelination - Knockout	Brain
(Hametner et al., 2018)	R2*, T1, QSM	Histology - LFB	Human	Vascular diseases	Brain
(Praet et al., 2018)	MK, RK, AK, FA, MD, RD, AD	Immunohistochemistry - MBP	Animal - Mouse	Amyloidosis	Brain
(Wendel et al., 2018)	FA, AD, RD, MD	Immunohistochemistry - MBP	Animal - Mouse	Traumatic brain injury	Brain
(West et al., 2018)	MPF, MWF, MVF-T2, MVF-MT	EM - Myelin fraction	Animal - Mouse	Demyelination - Knockout	Brain

(Yano et al., 2018)	FA, RD, MD	Immunohistochemistry - PLP	Animal - Mouse	Demyelination - Cuprizone	Brain
(Abe et al., 2019)	FA, RD, AD	Microscopy - Myelin thickness	Animal - Mouse	Optogenetic stimulation	Brain
(Duhamel et al., 2019)	ihMTR, MTR	Microscopy - Fluorescence	Animal - Mouse	Healthy	Brain
(M. Khodanovich et al., 2019)	MPF	Immunohistochemistry - MBP	Animal - Mouse	Demyelination - Cuprizone	Brain
(Mollink et al., 2019)	FA	Immunohistochemistry - MBP	Human	Amyotrophic lateral sclerosis	Brain
(Peters et al., 2019)	FA, MD	Histology - LFB	Human	Tuberous sclerosis complex	Brain
(Pol et al., 2019)	QSM, FA, MD	Histology - Solochrome	Animal - Mouse	Healthy	Brain
(Soustelle et al., 2019)	MPF, RD, MWF, rSPF	Immunohistochemistry - MBP	Animal - Mouse	Demyelination - Cuprizone	Brain
(Guglielmetti et al., 2020)	MTR, MTR-UTE	Immunohistochemistry - MBP	Animal - Mouse	Healthy	Brain

Supplementary material

To reproduce our results, we provided as supplementary material:

- A spreadsheet (database.xlsx) in xlsx format containing all the data and details collected for the studies considered in this systematic review;
- A multimedia file (interactive_figures.html) in HTML format containing an interactive version of the figures in this manuscript plus additional ones;
- A Jupyter notebook (interactive_figures.ipynb) in ipynb format containing the Python code used to process the data, run the analyses and generate all the figures.

In order to execute the notebook, the Python (3.7) and R (3.6) interpreters are required, as well as the R packages metafor (2.4) and multcomp (1.4), and the following Python packages:

- numpy (1.18.4);
- pandas (0.25.3);
- plotly (4.8.1);
- rpy2 (3.3.4);
- xlrd (1.2.0).

The notebook assumes that the spreadsheet is in the same path as the notebook itself. More details are provided at the following link:
https://github.com/matteomancini/myelin-meta-analysis

References

Abe, Y., Komaki, Y., Seki, F., Shibata, S., Okano, H., & Tanaka, K. F. (2019). Correlative study using structural MRI and super-resolution microscopy to detect structural alterations induced by long-term optogenetic stimulation of striatal medium spiny neurons. *Neurochem Int, 125*, 163-174. doi:10.1016/j.neuint.2019.02.017

Aojula, A., Botfield, H., McAllister, J. P., 2nd, Gonzalez, A. M., Abdullah, O., Logan, A., & Sinclair, A. (2016). Diffusion tensor imaging with direct cytopathological validation: characterisation of decorin treatment in experimental juvenile communicating hydrocephalus. *Fluids Barriers CNS, 13*(1), 9. doi:10.1186/s12987-016-0033-2

Beaulieu, C. (2002). The basis of anisotropic water diffusion in the nervous system – a technical review. *NMR in Biomedicine, 15*(7-8), 435-455. doi:10.1002/nbm.782

Beaulieu, C. (2009). CHAPTER 6 - The Biological Basis of Diffusion Anisotropy. In H. Johansen-Berg & T. E. J. Behrens (Eds.), *Diffusion MRI* (pp. 105-126). San Diego: Academic Press.

Beckmann, N., Giorgetti, E., Neuhaus, A., Zurbruegg, S., Accart, N., Smith, P., . . . Shimshek, D. R. (2018). Brain region-specific enhancement of remyelination and prevention of demyelination by the CSF1R kinase inhibitor BLZ945. *Acta Neuropathol Commun, 6*(1), 9. doi:10.1186/s40478-018-0510-8

Berman, S., West, K. L., Does, M. D., Yeatman, J. D., & Mezer, A. A. (2018). Evaluating g-ratio weighted changes in the corpus callosum as a function of age and sex. *Neuroimage, 182*, 304-313. doi:10.1016/j.neuroimage.2017.06.076

Cercignani, M., Dowell, N. G., & Tofts, P. S. (2018). *Quantitative MRI of the brain* (2nd edition ed.). Boca Raton: CRC Press.

Chandran, P., Upadhyay, J., Markosyan, S., Lisowski, A., Buck, W., Chin, C. L., . . . Day, M. (2012). Magnetic resonance imaging and histological evidence for the blockade of cuprizone-induced demyelination in C57BL/6 mice. *Neuroscience, 202*, 446-453. doi:10.1016/j.neuroscience.2011.10.051

Chang, E. H., Argyelan, M., Aggarwal, M., Chandon, T. S., Karlsgodt, K. H., Mori, S., & Malhotra, A. K. (2017). Diffusion tensor imaging measures of white matter compared to myelin basic protein immunofluorescence in tissue cleared intact brains. *Data Brief, 10*, 438-443. doi:10.1016/j.dib.2016.12.018

Chen, H. S., Holmes, N., Liu, J., Tetzlaff, W., & Kozlowski, P. (2017). Validating myelin water imaging with transmission electron microscopy in a rat spinal cord injury model. *Neuroimage, 153*, 122-130. doi:10.1016/j.neuroimage.2017.03.065

Cohen-Adad, J. (2018). Microstructural imaging in the spinal cord and validation strategies. *Neuroimage, 182*, 169-183. doi:10.1016/j.neuroimage.2018.04.009

Cohen-Adad, J., & Wheeler-Kingshott, C. A. (2014). *Quantitative MRI of the spinal cord*: Academic Press.

Does, M. D. (2018). Inferring brain tissue composition and microstructure via MR relaxometry. *Neuroimage, 182*, 136-148. doi:https://doi.org/10.1016/j.neuroimage.2017.12.087

Does, M. D., & Gore, J. C. (2000). Rapid Acquisition Transverse Relaxometric Imaging. *Journal of Magnetic Resonance, 147*(1), 116-120. doi:https://doi.org/10.1006/jmre.2000.2168

Du, J., Takahashi, A. M., Bydder, M., Chung, C. B., & Bydder, G. M. (2009). Ultrashort TE imaging with off-resonance saturation contrast (UTE-OSC). *Magnetic Resonance in Medicine, 62*(2), 527-531. doi:10.1002/mrm.22007

Duhamel, G., Prevost, V. H., Cayre, M., Hertanu, A., McHinda, S., Carvalho, V. N., . . . Girard, O. M. (2019). Validating the sensitivity of inhomogeneous magnetization transfer (ihMT) MRI to myelin with fluorescence microscopy. *Neuroimage, 199*, 289-303. doi:10.1016/j.neuroimage.2019.05.061

Dula, A. N., Gochberg, D. F., Valentine, H. L., Valentine, W. M., & Does, M. D. (2010). Multiexponential T2, magnetization transfer, and quantitative histology in white matter tracts of rat spinal cord. *Magnetic Resonance in Medicine, 63*(4), 902-909. doi:10.1002/mrm.22267

Fatemi, A., Wilson, M. A., Phillips, A. W., McMahon, M. T., Zhang, J., Smith, S. A., . . . Johnston, M. V. (2011). In vivo magnetization transfer MRI shows dysmyelination in an ischemic mouse model of periventricular leukomalacia. *J Cereb Blood Flow Metab, 31*(10), 2009-2018. doi:10.1038/jcbfm.2011.68

Feinberg, D. A., & Oshio, K. (1991). GRASE (gradient- and spin-echo) MR imaging: a new fast clinical imaging technique. *Radiology, 181*(2), 597-602. doi:10.1148/radiology.181.2.1924811

Fields, R. D. (2015). A new mechanism of nervous system plasticity: activity-dependent myelination. *Nature Reviews Neuroscience, 16*(12), 756-767. doi:10.1038/nrn4023

Fjaer, S., Bo, L., Lundervold, A., Myhr, K. M., Pavlin, T., Torkildsen, O., & Wergeland, S. (2013). Deep gray matter demyelination detected by magnetization transfer ratio in the cuprizone model. *PLoS One, 8*(12), e84162. doi:10.1371/journal.pone.0084162

Fjaer, S., Bo, L., Myhr, K. M., Torkildsen, O., & Wergeland, S. (2015). Magnetization transfer ratio does not correlate to myelin content in the brain in the MOG-EAE mouse model. *Neurochem Int, 83-84*, 28-40. doi:10.1016/j.neuint.2015.02.006

Guglielmetti, C., Boucneau, T., Cao, P., Van der Linden, A., Larson, P. E. Z., & Chaumeil, M. M. (2020). Longitudinal evaluation of demyelinated lesions in a multiple sclerosis model using ultrashort echo time magnetization transfer (UTE-MT) imaging. *Neuroimage, 208*, 116415. doi:10.1016/j.neuroimage.2019.116415

Hakkarainen, H., Sierra, A., Mangia, S., Garwood, M., Michaeli, S., Grohn, O., & Liimatainen, T. (2016). MRI relaxation in the presence of fictitious fields correlates with myelin content in normal rat brain. *Magn Reson Med, 75*(1), 161-168. doi:10.1002/mrm.25590

Hametner, S., Endmayr, V., Deistung, A., Palmrich, P., Prihoda, M., Haimburger, E., . . . Grabner, G. (2018). The influence of brain iron and myelin on magnetic susceptibility and effective transverse relaxation - A biochemical and histological validation study. *Neuroimage, 179*, 117-133. doi:10.1016/j.neuroimage.2018.06.007

Harkins, K. D., Dula, A. N., & Does, M. D. (2012). Effect of intercompartmental water exchange on the apparent myelin water fraction in multiexponential T2 measurements of rat spinal cord. *Magnetic Resonance in Medicine, 67*(3), 793-800. doi:10.1002/mrm.23053

Harkins, K. D., Valentine, W. M., Gochberg, D. F., & Does, M. D. (2013). In-vivo multi-exponential T2, magnetization transfer and quantitative histology in a rat model of intramyelinic edema. *Neuroimage Clin, 2*, 810-817. doi:10.1016/j.nicl.2013.06.007

Higgins, J. P. T., & Thompson, S. G. (2002). Quantifying heterogeneity in a meta-analysis. *Statistics in Medicine, 21*(11), 1539-1558. doi:10.1002/sim.1186

Höftberger, R., & Lassmann, H. (2018). Chapter 19 - Inflammatory demyelinating diseases of the central nervous system. In G. G. Kovacs & I. Alafuzoff (Eds.), *Handbook of Clinical Neurology* (Vol. 145, pp. 263-283): Elsevier.

Janve, V. A., Zu, Z., Yao, S. Y., Li, K., Zhang, F. L., Wilson, K. J., . . . Gochberg, D. F. (2013). The radial diffusivity and magnetization transfer pool size ratio are sensitive markers for demyelination in a rat model of type III multiple sclerosis (MS) lesions. *Neuroimage, 74*, 298-305. doi:10.1016/j.neuroimage.2013.02.034

Jelescu, I. O., Zurek, M., Winters, K. V., Veraart, J., Rajaratnam, A., Kim, N. S., . . . Fieremans, E. (2016). In vivo quantification of demyelination and recovery using compartment-specific diffusion MRI metrics validated by electron microscopy. *Neuroimage, 132*, 104-114. doi:10.1016/j.neuroimage.2016.02.004

Jito, J., Nakasu, S., Ito, R., Fukami, T., Morikawa, S., & Inubushi, T. (2008). Maturational changes in diffusion anisotropy in the rat corpus callosum: comparison with quantitative histological evaluation. *J Magn Reson Imaging, 28*(4), 847-854. doi:10.1002/jmri.21496

Kelm, N. D., West, K. L., Carson, R. P., Gochberg, D. F., Ess, K. C., & Does, M. D. (2016). Evaluation of diffusion kurtosis imaging in ex vivo hypomyelinated mouse brains. *Neuroimage, 124*(Pt A), 612-626. doi:10.1016/j.neuroimage.2015.09.028

Khodanovich, M., Pishchelko, A., Glazacheva, V., Pan, E., Akulov, A., Svetlik, M., . . . Yarnykh, V. (2019). Quantitative Imaging of White and Gray Matter Remyelination in the Cuprizone Demyelination Model Using the Macromolecular Proton Fraction. *Cells, 8*(10). doi:10.3390/cells8101204

Khodanovich, M. Y., Sorokina, I. V., Glazacheva, V. Y., Akulov, A. E., Nemirovich-Danchenko, N. M., Romashchenko, A. V., . . . Yarnykh, V. L. (2017). Histological validation of fast macromolecular proton fraction mapping as a quantitative myelin imaging method in the cuprizone demyelination model. *Sci Rep, 7*, 46686. doi:10.1038/srep46686

Kozlowski, P., Raj, D., Liu, J., Lam, C., Yung, A. C., & Tetzlaff, W. (2008). Characterizing white matter damage in rat spinal cord with quantitative MRI and histology. *J Neurotrauma, 25*(6), 653-676. doi:10.1089/neu.2007.0462

Kozlowski, P., Rosicka, P., Liu, J., Yung, A. C., & Tetzlaff, W. (2014). In vivo longitudinal Myelin Water Imaging in rat spinal cord following dorsal column transection injury. *Magn Reson Imaging, 32*(3), 250-258. doi:10.1016/j.mri.2013.12.006

Laule, C., Kozlowski, P., Leung, E., Li, D. K., Mackay, A. L., & Moore, G. R. (2008). Myelin water imaging of multiple sclerosis at 7 T: correlations with histopathology. *Neuroimage, 40*(4), 1575-1580. doi:10.1016/j.neuroimage.2007.12.008

Laule, C., Leung, E., Li, D. K. B., Traboulsee, A. L., Paty, D. W., MacKay, A. L., & Moore, G. R. W. (2006). Myelin water imaging in multiple sclerosis: quantitative correlations with histopathology. *Multiple Sclerosis, 12*, 747-753. doi:10.1177/1352458506070928

Laule, C., & Moore, G. R. W. (2018). Myelin water imaging to detect demyelination and remyelination and its validation in pathology. *Brain Pathol, 28*(5), 750-764. doi:10.1111/bpa.12645

Laule, C., Vavasour, I. M., Kolind, S. H., Li, D. K. B., Traboulsee, T. L., Moore, G. R. W., & MacKay, A. L. (2007). Magnetic Resonance Imaging of Myelin. *Neurotherapeutics, 4*(3), 460-484. doi:10.1016/j.nurt.2007.05.004

Laule, C., Vavasour, I. M., Leung, E., Li, D. K., Kozlowski, P., Traboulsee, A. L., . . . Moore, G. R. (2011). Pathological basis of diffusely abnormal white matter: insights from magnetic resonance imaging and histology. *Mult Scler, 17*(2), 144-150. doi:10.1177/1352458510384008

Lehman, E. L. (1999). *Elements of large-sample theory*. New York: Springer.

Lehto, L. J., Albors, A. A., Sierra, A., Tolppanen, L., Eberly, L. E., Mangia, S., . . . Grohn, O. (2017). Lysophosphatidyl Choline Induced Demyelination in Rat Probed by Relaxation along a Fictitious Field in High Rank Rotating Frame. *Front Neurosci, 11*, 433. doi:10.3389/fnins.2017.00433

Lehto, L. J., Sierra, A., & Grohn, O. (2017). Magnetization transfer SWIFT MRI consistently detects histologically verified myelin loss in the thalamocortical pathway after a traumatic brain injury in rat. *NMR Biomed, 30*(2). doi:10.1002/nbm.3678

Mackay, A., Whittall, K., Adler, J., Li, D., Paty, D., & Graeb, D. (1994). In vivo visualization of myelin water in brain by magnetic resonance. *Magnetic Resonance in Medicine, 31*(6), 673-677. doi:10.1002/mrm.1910310614

MacKay, A. L., & Laule, C. (2016). Magnetic Resonance of Myelin Water: An in vivo Marker for Myelin. *Brain Plast, 2*(1), 71-91. doi:10.3233/BPL-160033

Mollink, J., Hiemstra, M., Miller, K. L., Huszar, I. N., Jenkinson, M., Raaphorst, J., . . . van Cappellen van Walsum, A. M. (2019). White matter changes in the perforant path area in patients with amyotrophic lateral sclerosis. *Neuropathol Appl Neurobiol, 45*(6), 570-585. doi:10.1111/nan.12555

Nave, K. A., & Werner, H. B. (2014). Myelination of the nervous system: mechanisms and functions. *Annu Rev Cell Dev Biol, 30*, 503-533. doi:10.1146/annurev-cellbio-100913-013101

Odrobina, E. E., Lam, T. Y., Pun, T., Midha, R., & Stanisz, G. J. (2005). MR properties of excised neural tissue following experimentally induced demyelination. *NMR Biomed, 18*(5), 277-284. doi:10.1002/nbm.951

Peters, J. M., Struyven, R. R., Prohl, A. K., Vasung, L., Stajduhar, A., Taquet, M., . . . Warfield, S. K. (2019). White matter mean diffusivity correlates with myelination in tuberous sclerosis complex. *Ann Clin Transl Neurol, 6*(7), 1178-1190. doi:10.1002/acn3.793

Petiet, A., Adanyeguh, I., Aigrot, M. S., Poirion, E., Nait-Oumesmar, B., Santin, M., & Stankoff, B. (2019). Ultrahigh field imaging of myelin disease models: Toward specific markers of myelin integrity? *J Comp Neurol, 527*(13), 2179-2189. doi:10.1002/cne.24598

Pol, S., Sveinsson, M., Sudyn, M., Babek, N., Siebert, D., Bertolino, N., . . . Zivadinov, R. (2019). Teriflunomide's Effect on Glia in Experimental Demyelinating Disease: A Neuroimaging and Histologic Study. *J Neuroimaging, 29*(1), 52-61. doi:10.1111/jon.12561

Praet, J., Manyakov, N. V., Muchene, L., Mai, Z., Terzopoulos, V., de Backer, S., . . . Verhoye, M. (2018). Diffusion kurtosis imaging allows the early detection and longitudinal follow-up of amyloid-beta-induced pathology. *Alzheimers Res Ther, 10*(1), 1. doi:10.1186/s13195-017-0329-8

Prasloski, T., Rauscher, A., MacKay, A. L., Hodgson, M., Vavasour, I. M., Laule, C., & Mädler, B. (2012). Rapid whole cerebrum myelin water imaging using a 3D GRASE sequence. *Neuroimage, 63*(1), 533-539. doi:https://doi.org/10.1016/j.neuroimage.2012.06.064

Pun, T. W. C., Odrobina, E., Xu, Q. G., Lam, T. Y. J., Munro, C. A., Midha, R., & Stanisz, G. J. (2005). Histological and magnetic resonance analysis of sciatic nerves in the tellurium model of neuropathy. *Journal of the Peripheral Nervous System, 10*(1), 38-46. doi:10.1111/j.1085-9489.2005.10107.x

Raudenbush, S. W. (2009). Analyzing effect sizes: Random-effects models. In *The handbook of research synthesis and meta-analysis, 2nd ed.* (pp. 295-315). New York, NY, US: Russell Sage Foundation.

Reeves, C., Tachrount, M., Thomas, D., Michalak, Z., Liu, J., Ellis, M., . . . Thom, M. (2016). Combined Ex Vivo 9.4T MRI and Quantitative Histopathological Study in Normal and

Pathological Neocortical Resections in Focal Epilepsy. *Brain Pathol, 26*(3), 319-333. doi:10.1111/bpa.12298

Rooney, W. D., Johnson, G., Li, X., Cohen, E. R., Kim, S.-G., Ugurbil, K., & Springer Jr., C. S. (2007). Magnetic field and tissue dependencies of human brain longitudinal 1H2O relaxation in vivo. *Magnetic Resonance in Medicine, 57*(2), 308-318. doi:10.1002/mrm.21122

Sampaio-Baptista, C., & Johansen-Berg, H. (2017). White Matter Plasticity in the Adult Brain. *Neuron, 96*(6), 1239-1251. doi:10.1016/j.neuron.2017.11.026

Schmierer, K., Parkes, H. G., So, P. W., An, S. F., Brandner, S., Ordidge, R. J., . . . Miller, D. H. (2010). High field (9.4 Tesla) magnetic resonance imaging of cortical grey matter lesions in multiple sclerosis. *Brain, 133*(Pt 3), 858-867. doi:10.1093/brain/awp335

Schmierer, K., Scaravilli, F., Altmann, D. R., Barker, G. J., & Miller, D. H. (2004). Magnetization transfer ratio and myelin in postmortem multiple sclerosis brain. *Ann Neurol, 56*(3), 407-415. doi:10.1002/ana.20202

Schmierer, K., Tozer, D. J., Scaravilli, F., Altmann, D. R., Barker, G. J., Tofts, P. S., & Miller, D. H. (2007). Quantitative magnetization transfer imaging in postmortem multiple sclerosis brain. *J Magn Reson Imaging, 26*(1), 41-51. doi:10.1002/jmri.20984

Schmierer, K., Wheeler-Kingshott, C. A., Boulby, P. A., Scaravilli, F., Altmann, D. R., Barker, G. J., . . . Miller, D. H. (2007). Diffusion tensor imaging of post mortem multiple sclerosis brain. *Neuroimage, 35*(2), 467-477. doi:10.1016/j.neuroimage.2006.12.010

Schmierer, K., Wheeler-Kingshott, C. A., Tozer, D. J., Boulby, P. A., Parkes, H. G., Yousry, T. A., . . . Miller, D. H. (2008). Quantitative magnetic resonance of postmortem multiple sclerosis brain before and after fixation. *Magn Reson Med, 59*(2), 268-277. doi:10.1002/mrm.21487

Seehaus, A., Roebroeck, A., Bastiani, M., Fonseca, L., Bratzke, H., Lori, N., . . . Galuske, R. (2015). Histological validation of high-resolution DTI in human post mortem tissue. *Front Neuroanat, 9*, 98. doi:10.3389/fnana.2015.00098

Sled, J. G. (2018). Modelling and interpretation of magnetization transfer imaging in the brain. *Neuroimage, 182*, 128-135. doi:https://doi.org/10.1016/j.neuroimage.2017.11.065

Soustelle, L., Antal, M. C., Lamy, J., Rousseau, F., Armspach, J. P., & Loureiro de Sousa, P. (2019). Correlations of quantitative MRI metrics with myelin basic protein (MBP) staining in a murine model of demyelination. *NMR Biomed, 32*(9), e4116. doi:10.1002/nbm.4116

Stanisz, G. J., Kecojevic, A., Bronskill, M. J., & Henkelman, R. M. (1999). Characterizing white matter with magnetization transfer and T2. *Magnetic Resonance in Medicine, 42*(6), 1128-1136. doi:10.1002/(sici)1522-2594(199912)42:6<1128::Aid-mrm18>3.0.Co;2-9

Stanisz, G. J., Webb, S., Munro, C. A., Pun, T., & Midha, R. (2004). MR properties of excised neural tissue following experimentally induced inflammation. *Magnetic Resonance in Medicine, 51*(3), 473-479. doi:10.1002/mrm.20008

Takagi, T., Nakamura, M., Yamada, M., Hikishima, K., Momoshima, S., Fujiyoshi, K., . . . Okano, H. (2009). Visualization of peripheral nerve degeneration and regeneration: monitoring with diffusion tensor tractography. *Neuroimage, 44*(3), 884-892. doi:10.1016/j.neuroimage.2008.09.022

Tardif, C. L., Bedell, B. J., Eskildsen, S. F., Collins, D. L., & Pike, G. B. (2012). Quantitative magnetic resonance imaging of cortical multiple sclerosis pathology. *Mult Scler Int, 2012*, 742018. doi:10.1155/2012/742018

Thiessen, J. D., Zhang, Y., Zhang, H., Wang, L., Buist, R., Del Bigio, M. R., . . . Martin, M. (2013). Quantitative MRI and ultrastructural examination of the cuprizone mouse model of demyelination. *NMR Biomed, 26*(11), 1562-1581. doi:10.1002/nbm.2992

Tu, T. W., Williams, R. A., Lescher, J. D., Jikaria, N., Turtzo, L. C., & Frank, J. A. (2016). Radiological-pathological correlation of diffusion tensor and magnetization transfer imaging in a closed head traumatic brain injury model. *Ann Neurol, 79*(6), 907-920. doi:10.1002/ana.24641

Turati, L., Moscatelli, M., Mastropietro, A., Dowell, N. G., Zucca, I., Erbetta, A., . . . Minati, L. (2015). In vivo quantitative magnetization transfer imaging correlates with histology during de- and remyelination in cuprizone-treated mice. *NMR Biomed, 28*(3), 327-337. doi:10.1002/nbm.3253

Turner, R. (2019). Myelin and Modeling: Bootstrapping Cortical Microcircuits. *Front Neural Circuits, 13*, 34. doi:10.3389/fncir.2019.00034

Underhill, H. R., Rostomily, R. C., Mikheev, A. M., Yuan, C., & Yarnykh, V. L. (2011). Fast bound pool fraction imaging of the in vivo rat brain: association with myelin content and validation in the C6 glioma model. *Neuroimage, 54*(3), 2052-2065. doi:10.1016/j.neuroimage.2010.10.065

van Tilborg, E., Achterberg, E. J. M., van Kammen, C. M., van der Toorn, A., Groenendaal, F., Dijkhuizen, R. M., . . . Nijboer, C. H. A. (2018). Combined fetal inflammation and postnatal hypoxia causes myelin deficits and autism-like behavior in a rat model of diffuse white matter injury. *Glia, 66*(1), 78-93. doi:10.1002/glia.23216

Varma, G., Duhamel, G., de Bazelaire, C., & Alsop, D. C. (2015). Magnetization transfer from inhomogeneously broadened lines: A potential marker for myelin. *Magnetic Resonance in Medicine, 73*(2), 614-622. doi:10.1002/mrm.25174

Viechtbauer, W. (2010). Conducting Meta-Analyses in R with the metafor Package. *Journal of Statistical Software, 36*(3). doi:10.18637/jss.v036.i03

Wang, S., Wu, E. X., Cai, K., Lau, H. F., Cheung, P. T., & Khong, P. L. (2009). Mild hypoxic-ischemic injury in the neonatal rat brain: longitudinal evaluation of white matter using diffusion tensor MR imaging. *AJNR Am J Neuroradiol, 30*(10), 1907-1913. doi:10.3174/ajnr.A1697

Wang, X., Cusick, M. F., Wang, Y., Sun, P., Libbey, J. E., Trinkaus, K., . . . Song, S. K. (2014). Diffusion basis spectrum imaging detects and distinguishes coexisting subclinical inflammation, demyelination and axonal injury in experimental autoimmune encephalomyelitis mice. *NMR Biomed, 27*(7), 843-852. doi:10.1002/nbm.3129

Wang, Y., Sun, P., Wang, Q., Trinkaus, K., Schmidt, R. E., Naismith, R. T., . . . Song, S. K. (2015). Differentiation and quantification of inflammation, demyelination and axon injury or loss in multiple sclerosis. *Brain, 138*(Pt 5), 1223-1238. doi:10.1093/brain/awv046

Wei, H., Cao, P., Bischof, A., Henry, R. G., Larson, P. E. Z., & Liu, C. (2018). MRI gradient-echo phase contrast of the brain at ultra-short TE with off-resonance saturation. *Neuroimage, 175*, 1-11. doi:https://doi.org/10.1016/j.neuroimage.2018.03.066

Wendel, K. M., Lee, J. B., Affeldt, B. M., Hamer, M., Harahap-Carrillo, I. S., Pardo, A. C., & Obenaus, A. (2018). Corpus Callosum Vasculature Predicts White Matter Microstructure Abnormalities after Pediatric Mild Traumatic Brain Injury. *J Neurotrauma*. doi:10.1089/neu.2018.5670

West, K. L., Kelm, N. D., Carson, R. P., Gochberg, D. F., Ess, K. C., & Does, M. D. (2018). Myelin volume fraction imaging with MRI. *Neuroimage, 182*, 511-521. doi:10.1016/j.neuroimage.2016.12.067

Wu, Q. Z., Yang, Q., Cate, H. S., Kemper, D., Binder, M., Wang, H. X., . . . Egan, G. F. (2008). MRI identification of the rostral-caudal pattern of pathology within the corpus callosum in the cuprizone mouse model. *J Magn Reson Imaging, 27*(3), 446-453. doi:10.1002/jmri.21111

Yano, R., Hata, J., Abe, Y., Seki, F., Yoshida, K., Komaki, Y., . . . Tanaka, K. F. (2018). Quantitative temporal changes in DTI values coupled with histological properties in cuprizone-induced demyelination and remyelination. *Neurochem Int, 119*, 151-158. doi:10.1016/j.neuint.2017.10.004

Yarnykh, V. L. (2012). Fast macromolecular proton fraction mapping from a single off-resonance magnetization transfer measurement. *Magnetic Resonance in Medicine, 68*(1), 166-178. doi:10.1002/mrm.23224

Zaaraoui, W., Deloire, M., Merle, M., Girard, C., Raffard, G., Biran, M., . . . Dousset, V. (2008). Monitoring demyelination and remyelination by magnetization transfer imaging in the mouse brain at 9.4 T. *MAGMA, 21*(5), 357-362. doi:10.1007/s10334-008-0141-3

Zhang, J., Jones, M., DeBoy, C. A., Reich, D. S., Farrell, J. A., Hoffman, P. N., . . . Calabresi, P. A. (2009). Diffusion tensor magnetic resonance imaging of Wallerian degeneration in rat spinal cord after dorsal root axotomy. *J Neurosci, 29*(10), 3160-3171. doi:10.1523/JNEUROSCI.3941-08.2009

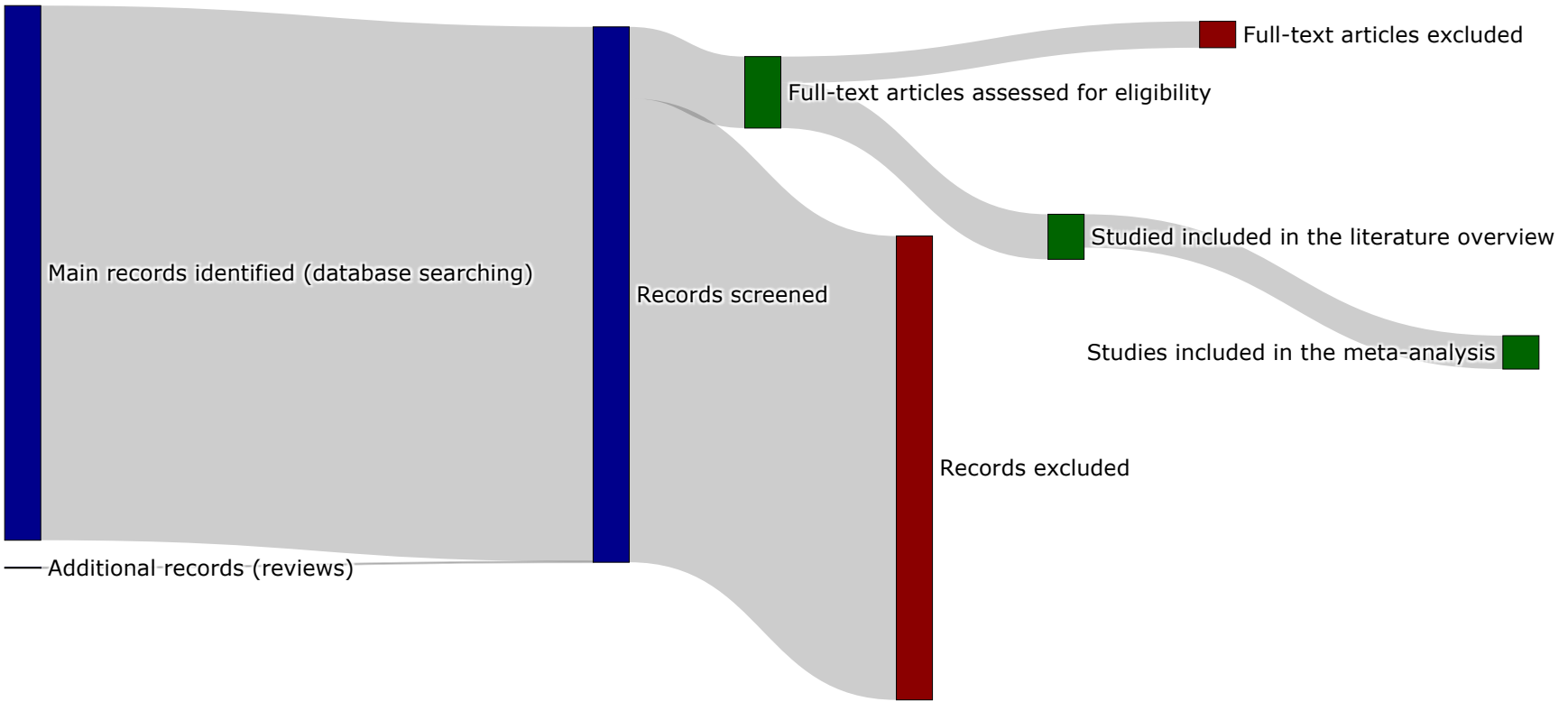
Main records identified (database searching)
Additional records (reviews)
Records screened
Full-text articles assessed for eligibility
Full-text articles excluded
Records excluded
Studied included in the literature overview
Studies included in the meta-analysis

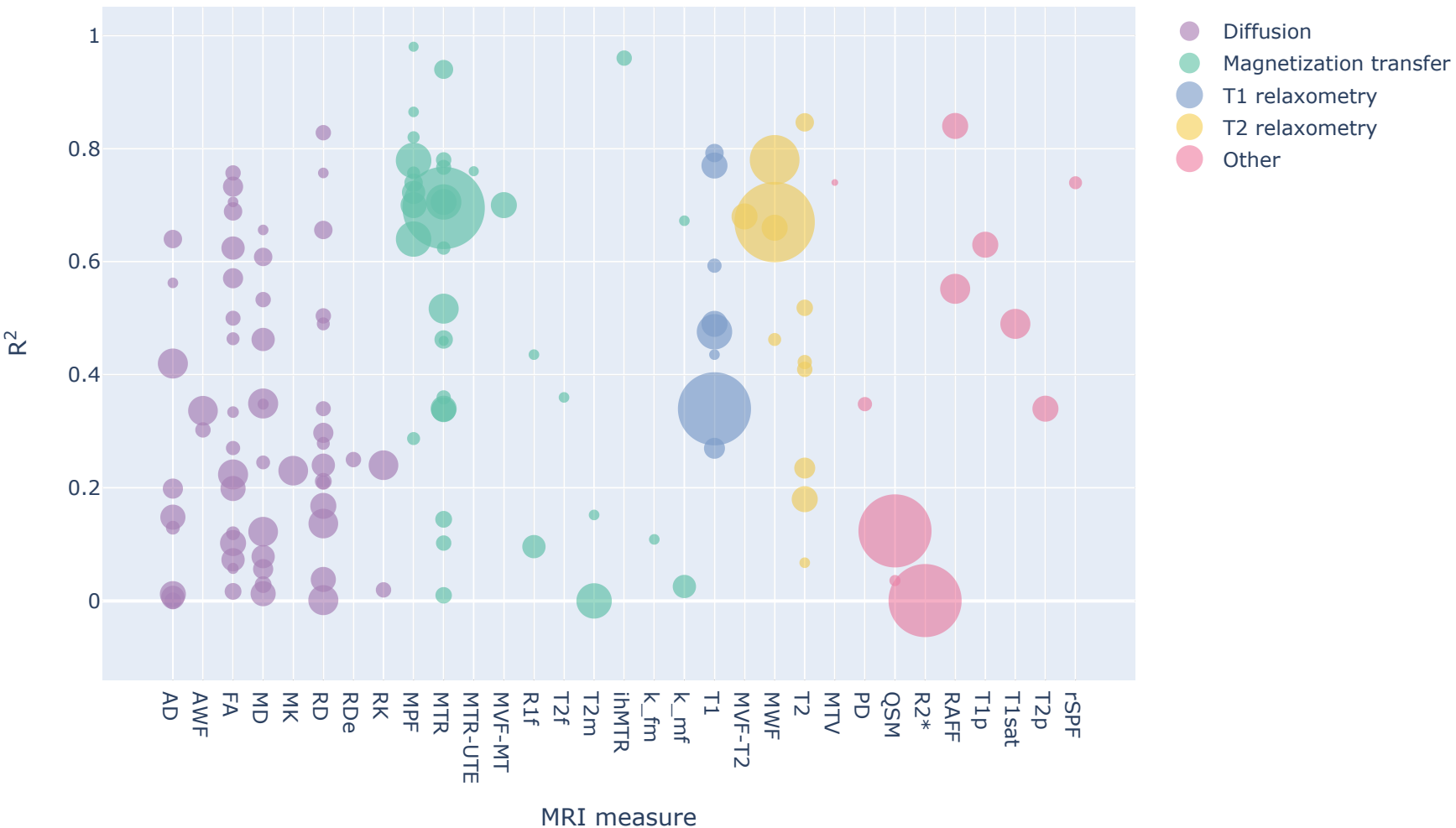
Diffusion
Magnetization transfer
T1 relaxometry
T2 relaxometry
Other
R2
1
0.8
0.6
0.4
0.2
0
AD
AWF
FA
MD
MK
RD
RDe
RK
MPF
MTR
MTR-UTE
MVF-MT
R1f
T2f
T2m
inMTR
k_fm
k_mf
T1
MVF-T2
MWF
T2
MTV
PD
QSM
R2*
RAFF
T1p
T1sat
T2p
rSPF
MRI measure

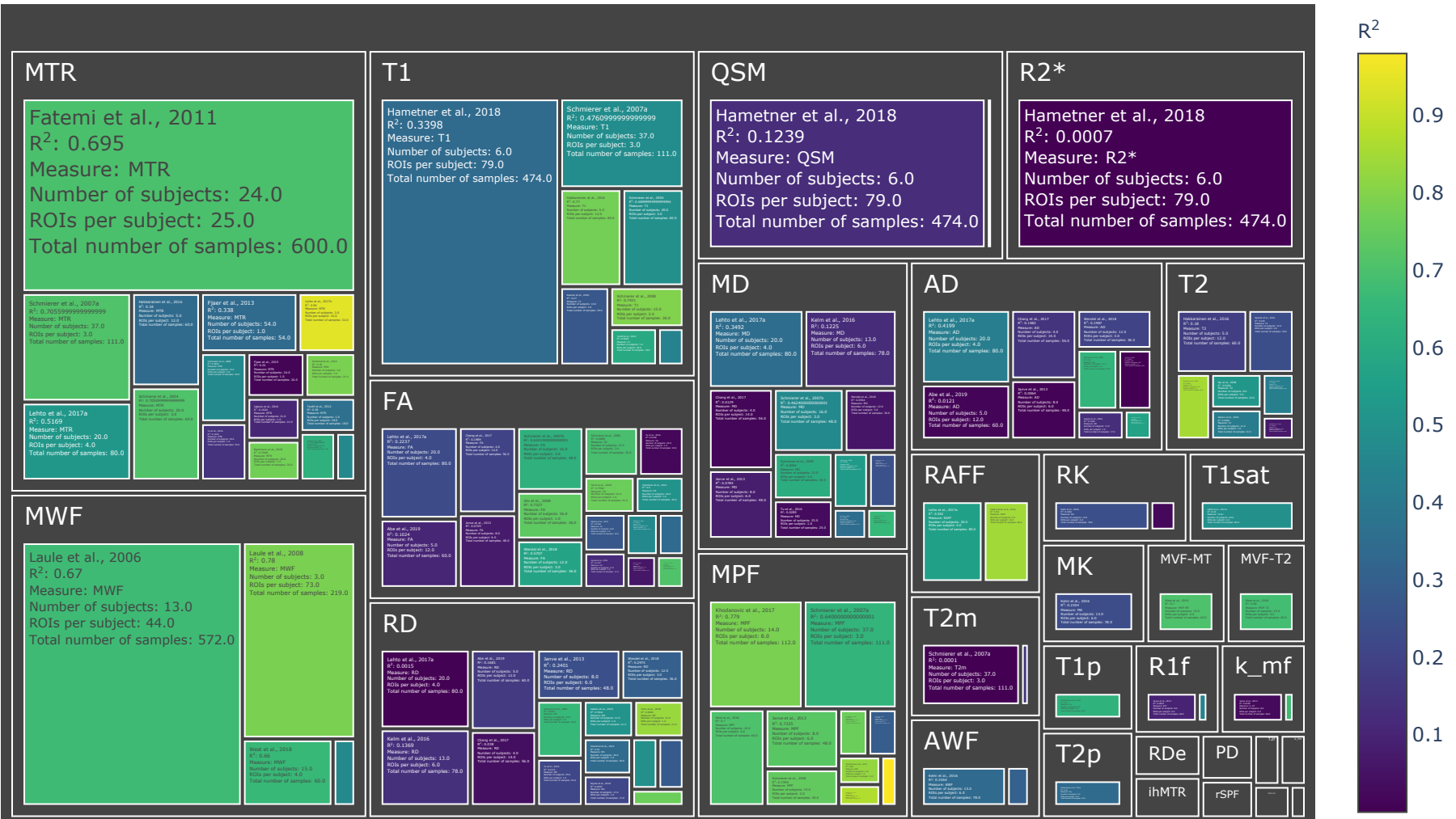
MTR
Fatemi et al., 2011
R2: 0.695
Measure: MTR
Number of subjects: 24.0
ROIs per subject: 25.0
Total number of samples: 600.0
Schmierer et al., 2007a
R2: 0.7055999999999999
Measure: MTR
Number of subjects: 37.0
ROIs per subject: 3.0
Total number of samples: 111.0
Fjaer et al., 2013
R2: 0.338
Measure: MTR
Number of subjects: 54.0
ROIs per subject: 1.0
Total number of samples: 54.0
Lehto et al., 2017a
R2: 0.5169
Measure: MTR
Number of subjects: 20.0
ROIs per subject: 4.0
Total number of samples: 80.0
MWF
Laule et al., 2006
R2: 0.67
Measure: MWF
Number of subjects: 13.0
ROIs per subject: 44.0
Total number of samples: 572.0
Laule et al., 2008
R2: 0.78
Measure: MWF
Number of subjects: 3.0
ROIs per subject: 73.0
Total number of samples: 219.0
West et al., 2018
R2: 0.66
Measure: MWF
Number of subjects: 15.0
ROIs per subject: 4.0
Total number of samples: 60.0
T1
Hametner et al., 2018
R2: 0.3398
Measure: T1
Number of subjects: 6.0
ROIs per subject: 79.0
Total number of samples: 474.0
Schmierer et al., 2007a
R2: 0.4760999999999999
Measure: T1
Number of subjects: 37.0
ROIs per subject: 3.0
Total number of samples: 111.0
FA
Lehto et al., 2017a
R2: 0.2237
Measure: FA
Number of subjects: 20.0
ROIs per subject: 4.0
Total number of samples: 80.0
Abe et al., 2019
R2: 0.1024
Measure: FA
Number of subjects: 5.0
ROIs per subject: 12.0
Total number of samples: 60.0
RD
Lehto et al., 2017a
R2: 0.0015
Measure: RD
Number of subjects: 20.0
ROIs per subject: 4.0
Total number of samples: 80.0
Kelm et al., 2016
R2: 0.1369
Measure: RD
Number of subjects: 13.0
ROIs per subject: 6.0
Total number of samples: 78.0
Janve et al., 2013
R2: 0.2401
Measure: RD
Number of subjects: 8.0
ROIs per subject: 6.0
Total number of samples: 48.0
QSM
Hametner et al., 2018
R2: 0.1239
Measure: QSM
Number of subjects: 6.0
ROIs per subject: 79.0
Total number of samples: 474.0
R2*
Hametner et al., 2018
R2: 0.0007
Measure: R2*
Number of subjects: 6.0
ROIs per subject: 79.0
Total number of samples: 474.0
MD
Lehto et al., 2017a
R2: 0.3492
Measure: MD
Number of subjects: 20.0
ROIs per subject: 4.0
Total number of samples: 80.0
Kelm et al., 2016
R2: 0.1225
Measure: MD
Number of subjects: 13.0
ROIs per subject: 6.0
Total number of samples: 78.0
MPF
Khodanovic et al., 2017
R2: 0.779
Measure: MPF
Number of subjects: 14.0
ROIs per subject: 8.0
Total number of samples: 112.0
Schmierer et al., 2007a
R2: 0.6400000000000001
Measure: MPF
Number of subjects: 37.0
ROIs per subject: 3.0
Total number of samples: 111.0
AD
Lehto et al., 2017a
R2: 0.4199
Measure: AD
Number of subjects: 20.0
ROIs per subject: 4.0
Total number of samples: 80.0
Abe et al., 2019
R2: 0.0121
Measure: AD
Number of subjects: 5.0
ROIs per subject: 12.0
Total number of samples: 60.0
T2
RAFF
RK
T1sat
MK
MVF-MT
MVF-T2
T2m
Schmierer et al., 2007a
R2: 0.0001
Measure: T2m
Number of subjects: 37.0
ROIs per subject: 3.0
Total number of samples: 111.0
T1p
R1f
k_mf
AWF
T2p
RDe
PD
ihMTR
rSPF
R2
0.9
0.8
0.7
0.6
0.5
0.4
0.3
0.2
0.1

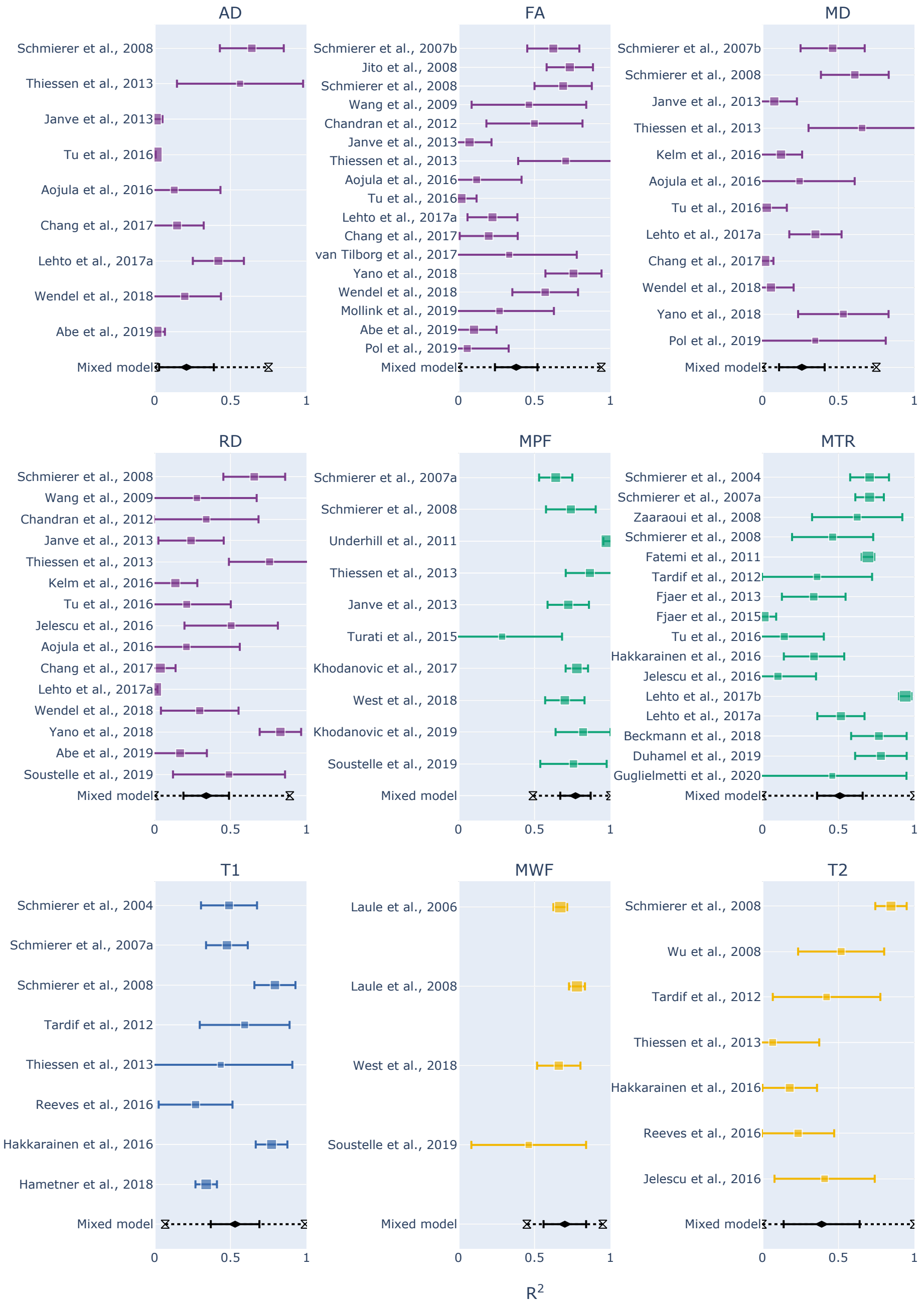
AD
Schmierer et al., 2008
Thiessen et al., 2013
Janve et al., 2013
Tu et al., 2016
Aojula et al., 2016
Chang et al., 2017
Lehto et al., 2017a
Wendel et al., 2018
Abe et al., 2019
Mixed model
0
0.5
1
FA
Schmierer et al., 2007b
Jito et al., 2008
Schmierer et al., 2008
Wang et al., 2009
Chandran et al., 2012
Janve et al., 2013
Thiessen et al., 2013
Aojula et al., 2016
Tu et al., 2016
Lehto et al., 2017a
Chang et al., 2017
van Tilborg et al., 2017
Yano et al., 2018
Wendel et al., 2018
Mollink et al., 2019
Abe et al., 2019
Pol et al., 2019
Mixed model
0
0.5
1
MD
Schmierer et al., 2007b
Schmierer et al., 2008
Janve et al., 2013
Thiessen et al., 2013
Kelm et al., 2016
Aojula et al., 2016
Tu et al., 2016
Lehto et al., 2017a
Chang et al., 2017
Wendel et al., 2018
Yano et al., 2018
Pol et al., 2019
Mixed model
0
0.5
1
RD
Schmierer et al., 2008
Wang et al., 2009
Chandran et al., 2012
Janve et al., 2013
Thiessen et al., 2013
Kelm et al., 2016
Tu et al., 2016
Jelescu et al., 2016
Aojula et al., 2016
Chang et al., 2017
Lehto et al., 2017a
Wendel et al., 2018
Yano et al., 2018
Abe et al., 2019
Soustelle et al., 2019
Mixed model
0
0.5
1
MPF
Schmierer et al., 2007a
Schmierer et al., 2008
Underhill et al., 2011
Thiessen et al., 2013
Janve et al., 2013
Turati et al., 2015
Khodanovic et al., 2017
West et al., 2018
Khodanovic et al., 2019
Soustelle et al., 2019
Mixed model
0
0.5
1
MTR
Schmierer et al., 2004
Schmierer et al., 2007a
Zaaraoui et al., 2008
Schmierer et al., 2008
Fatemi et al., 2011
Tardif et al., 2012
Fjaer et al., 2013
Fjaer et al., 2015
Tu et al., 2016
Hakkarainen et al., 2016
Jelescu et al., 2016
Lehto et al., 2017b
Lehto et al., 2017a
Beckmann et al., 2018
Duhamel et al., 2019
Guglielmetti et al., 2020
Mixed model
0
0.5
1
T1
Schmierer et al., 2004
Schmierer et al., 2007a
Schmierer et al., 2008
Tardif et al., 2012
Thiessen et al., 2013
Reeves et al., 2016
Hakkarainen et al., 2016
Hametner et al., 2018
Mixed model
0
0.5
1
MWF
Laule et al., 2006
Laule et al., 2008
West et al., 2018
Soustelle et al., 2019
Mixed model
0
0.5
1
T2
Schmierer et al., 2008
Wu et al., 2008
Tardif et al., 2012
Thiessen et al., 2013
Hakkarainen et al., 2016
Reeves et al., 2016
Jelescu et al., 2016
Mixed model
0
0.5
1
R^2

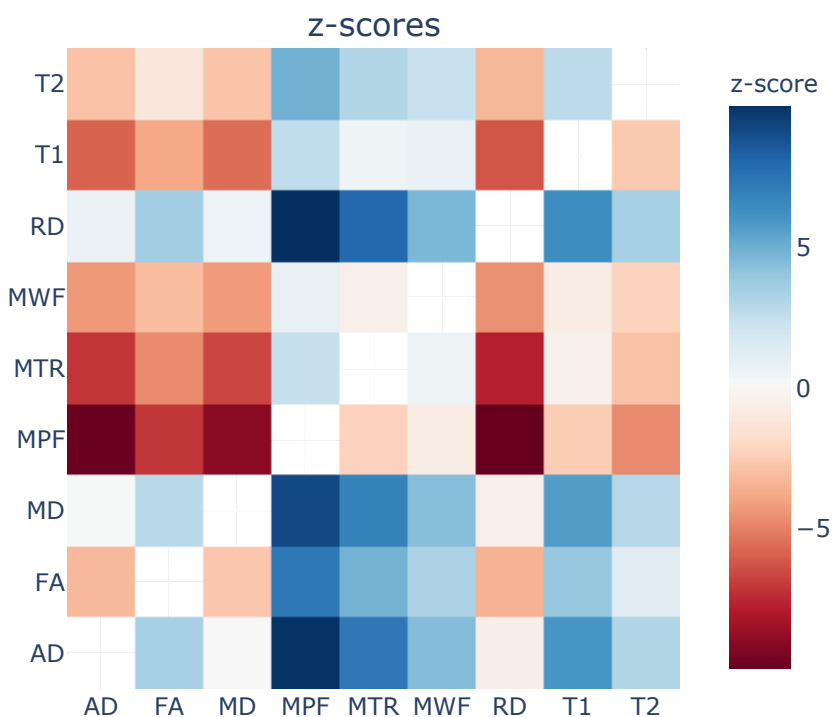
z-scores
T2
T1
RD
MWF
MTR
MPF
MD
FA
AD
AD
FA
MD
MPF
MTR
MWF
RD
T1
T2
z-score
5
0
−5

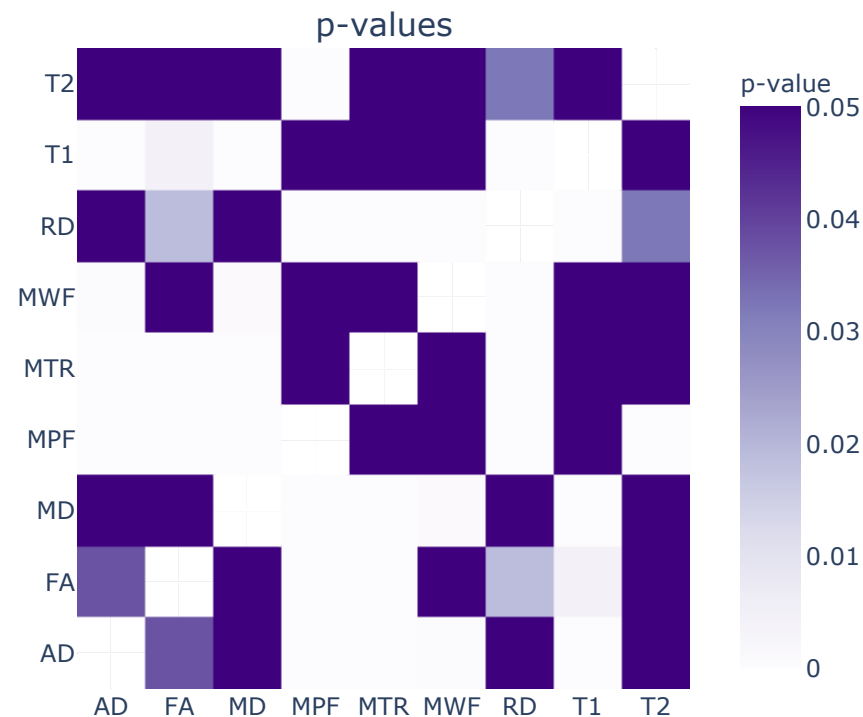
p-values
T2
T1
RD
MWF
MTR
MPF
MD
FA
AD
AD
FA
MD
MPF
MTR
MWF
RD
T1
T2
p-value
0.05
0.04
0.03
0.02
0.01
0

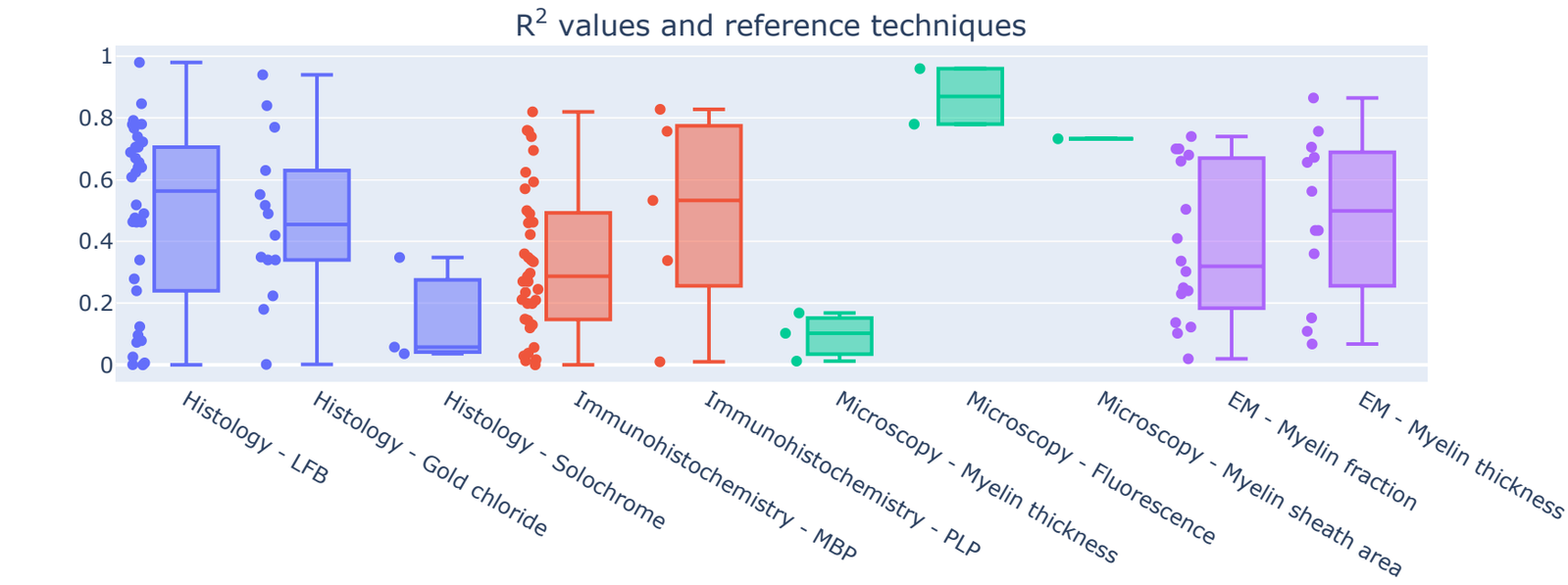
R2 values and reference techniques
1
0.8
0.6
0.4
0.2
0
Histology - LFB
Histology - Gold chloride
Histology - Solochrome
Immunohistochemistry - MBP
Immunohistochemistry - PLP
Microscopy - Myelin thickness
Microscopy - Fluorescence
Microscopy - Myelin sheath area
EM - Myelin fraction
EM - Myelin thickness

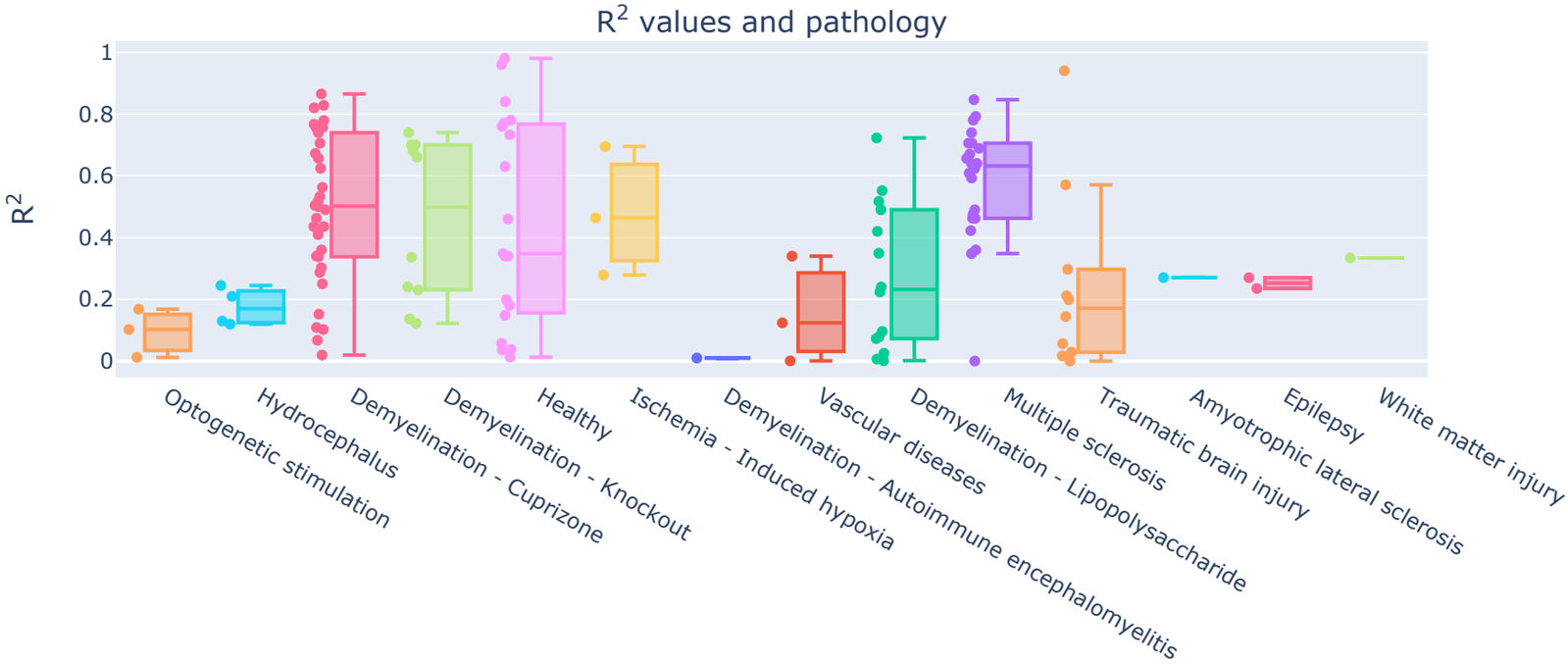
R2 values and pathology
R2
1
0.8
0.6
0.4
0.2
0
Optogenetic stimulation
Hydrocephalus
Demyelination - Cuprizone
Demyelination - Knockout
Healthy
Ischemia - Induced hypoxia
Demyelination - Autoimmune encephalomyelitis
Vascular diseases
Demyelination - Lipopolysaccharide
Multiple sclerosis
Traumatic brain injury
Amyotrophic lateral sclerosis
Epilepsy
White matter injury

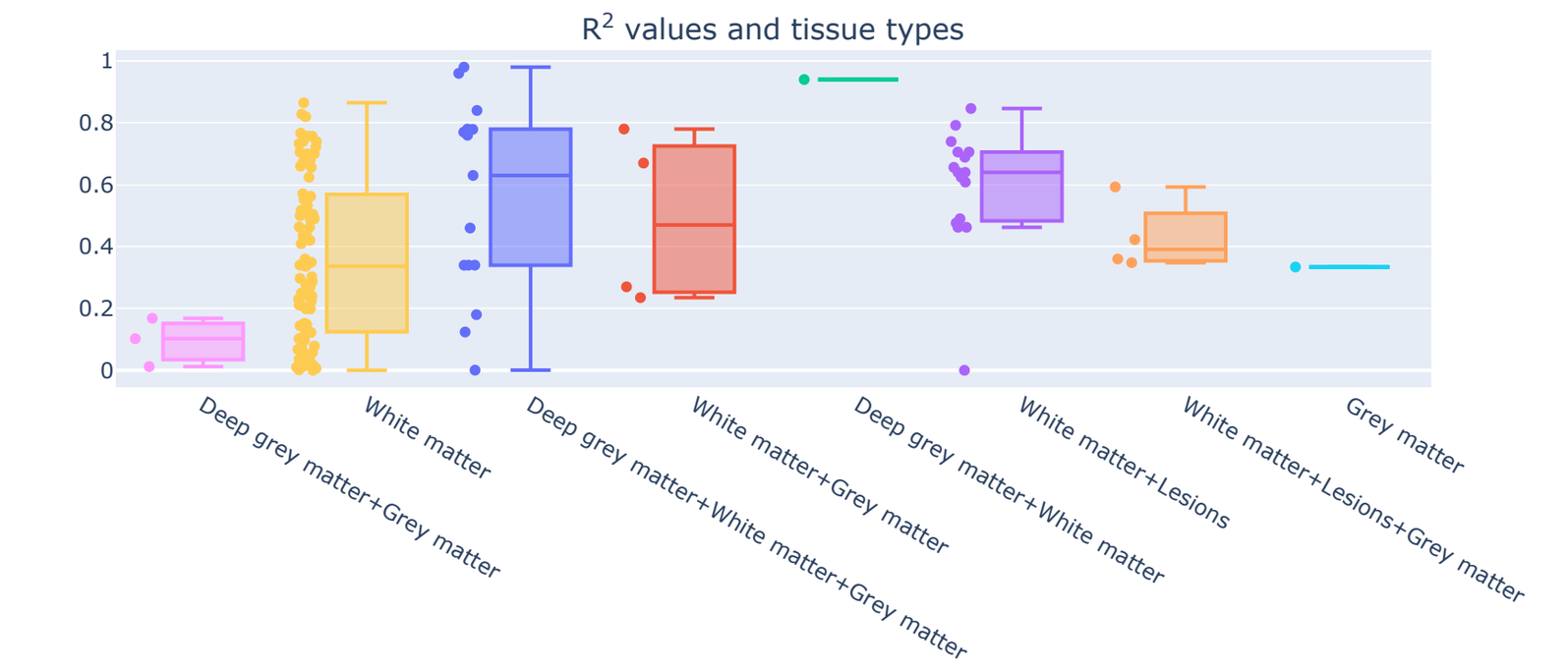
R2 values and tissue types
1
0.8
0.6
0.4
0.2
0
Deep grey matter+Grey matter
White matter
Deep grey matter+White matter+Grey matter
White matter+Grey matter
Deep grey matter+White matter
White matter+Lesions
White matter+Lesions+Grey matter
Grey matter